UNIVERSITETET I NORDLAND

MASTER THESIS

Compairing trophic positions of Mesozooplankton estimated by stable isotopes and biovolume spectrum theories

Nuwan A.L. De Silva

BI309F MSc in Marine Ecology
Faculty of Biosciences and Aquaculture
May 2014

CONTENTS

LIST OF TABLES

LIST OF FIGURES

ABSTRACT

Biovolume spectrum theory is now being used increasingly to represent the trophic structure of marine mesozooplankton communities, yet the ability of applying biovolume spectrum theory to indicate the trophic position of different mesozooplankton size groups remains untested using direct sampling methods such as stable isotope analyses. Therefore, this study has combined the estimations of trophic positions (TPs) using biovolume spectrum theory with stable nitrogen isotope ratios (δ^{15}N), allowed direct comparison of TPs estimates from both methods for different groups of zooplankton in relation to the states of the phytoplankton bloom and different water masses. Hydrographical and biological data were collected from the subpolar North Atlantic Ocean in March/April, 2013 using multinet, WP 2 net and a platform equipped with Laser Optical Plankton Counter, Conductivity temperature depth sensor and Fluorescence sensor. TPs estimates based on biovolume spectrum theory did not correspond to δ^{15}N estimates while producing relatively higher TPs compared to isotopic estimates. Several factors may explain these discrepancies between the two methods. A responsiveness of the biovolume spectrum to recycling processes driven by microbial community, that was not detected precisely by the stable isotope analyses could be identified as the most reasonable and straightforward factor for the observed discrepancies. Hence, a hypothetical model was developed to trace and evaluate these microbial based food web within zooplankton community. Model interpretation showed a microbial loop dominated zooplankton food web in the Labrador Sea surface water (LSSW) during the pre-bloom condition, while, less microbial influence to determine the zooplankton food web structure in Atlantic water (AtW) during the winter condition. Findings of the study, thus proved applying of biovolume spectrum theory to data obtained by LOPC as a high resolution method not only for estimation of TPs, but also to trace the influence of microbial processes for the sustainability of mesozooplankton communities.

1. INTRODUCTION

Accurate representation and description of trophic relationships are essential to a wide range of ecological studies (Vander Zanden et al., 1997). The concept of discrete trophic levels (i.e. grouping organisms by trophic level, producer = 1, herbivore = 2, predator =3) is commonly used in ecological   studies and has been used successfully in studies predicting contaminant bioaccumulation in top predators (Rasmussen et al., 1990; Cabana et al., 1994). Furthermore, trophic levels provide the framework for studies of cascading trophic interactions (Carpenter et al., 1985; Wooton and Power, 1993) and ecological energetics and efficiencies (Lindeman, 1942). However this categorical approach does not account for complex trophic interactions such as omnivory (Kling et al., 1992). Trophic position is a continuous variable that accounts for omnivory and better quantifies matter and energy flow within a food web (Kling et al., 1992; Vander Zanden & Rasmussen, 1996) and can be used as effective tool for assessing trophic interactions of highly dynamic marine zooplankton communities.

The structure of zooplankton communities plays a crucial role in determining the fate of primary production (Steinberg et al., 2008). Feeding by herbivorous mesozooplankton at the base of pelagic food webs links primary production and the microbial loop to higher trophic levels (Muñoz, 2007). However, all herbivorous mesozooplankton species are known to be opportunistic feeders i.e. omnivorous to some degree (Sommer & Sommer, 2006) depending on prey size and motility (Tiselius & Jonsson, 1990), turbulence (Saiz & Kioerboe, 1995), feeding strategy (Greene, 1988) and states of phytoplankton blooms (Meyer-Harms et al., 1999), therefore it is difficult to disentangle trophic relationships.

Fundamental to an understanding of the trophic structure of mesozooplankton is the knowledge of feeding relationships among species and their respective trophic positions through time and across space at the whole-community level (Muñoz, 2007). Traditionally trophic positions has

been estimated from gut contents analysis and provides detailed information on species' diets, but does no account for long-term patterns of mass transfer (Vander Zanden et al., 1997). Moreover, dietary analysis only reflects recent feeding history (Tieszen et al., 1983).

Stable isotope analyses is increasingly being used to calculate trophic relationships in aquatic systems (e.g., Post, 2002; Jardine et al., 2006). Stable isotope analysis has become an effective technique for elucidating energy flow pathways through food webs, examining trophic interactions and elucidating the trophic structure in an ecosystem (Peterson & Fry, 1987, Lajtha & Michener, 1994). The natural abundance of carbon and nitrogen stable isotopes in organisms indicates the sources for organic matter and nutrients, as well as their processing through the food web, because at each ascending trophic level (from prey to predator), there is an increase in the carbon isotope (δ^{13} C or $^{13}C/^{12}C$ ratio) content and nitrogen isotope (δ^{15} N or $^{15}N/^{14}N$ ratio) content of the organism due to selective metabolic loss of ^{12}C and ^{14}N during food assimilation (Layman et al., 2011). In the case of nitrogen isotope (δ^{15} N) there is a characteristic enrichment along the food web, i.e. the consumer is typically enriched by 3–4‰ relative to its diet (Peterson and Fry, 1987). Thus, allowing for determination of trophic position of species (Vander Zanden and Rassmusen, 2001). In contrast, carbon isotope (δ^{13} C) change little as carbon moves through food webs (Figure 1) (Rounick and Winterbourn 1986, Peterson and Fry 1987, France and Peters 1997) and, therefore, typically can be used to evaluate the ultimate sources of carbon for an organism when the isotopic signature of the sources are different (Post, 2002). Hence, stable isotope analyses can be a powerful approach and has been applied successfully in the field as well as natural tracer and trophic status survey of mesozooplankton species (e.g. Rolff , 2000, Rolff & Elmgren, 2000, Sommer et al., 2005).
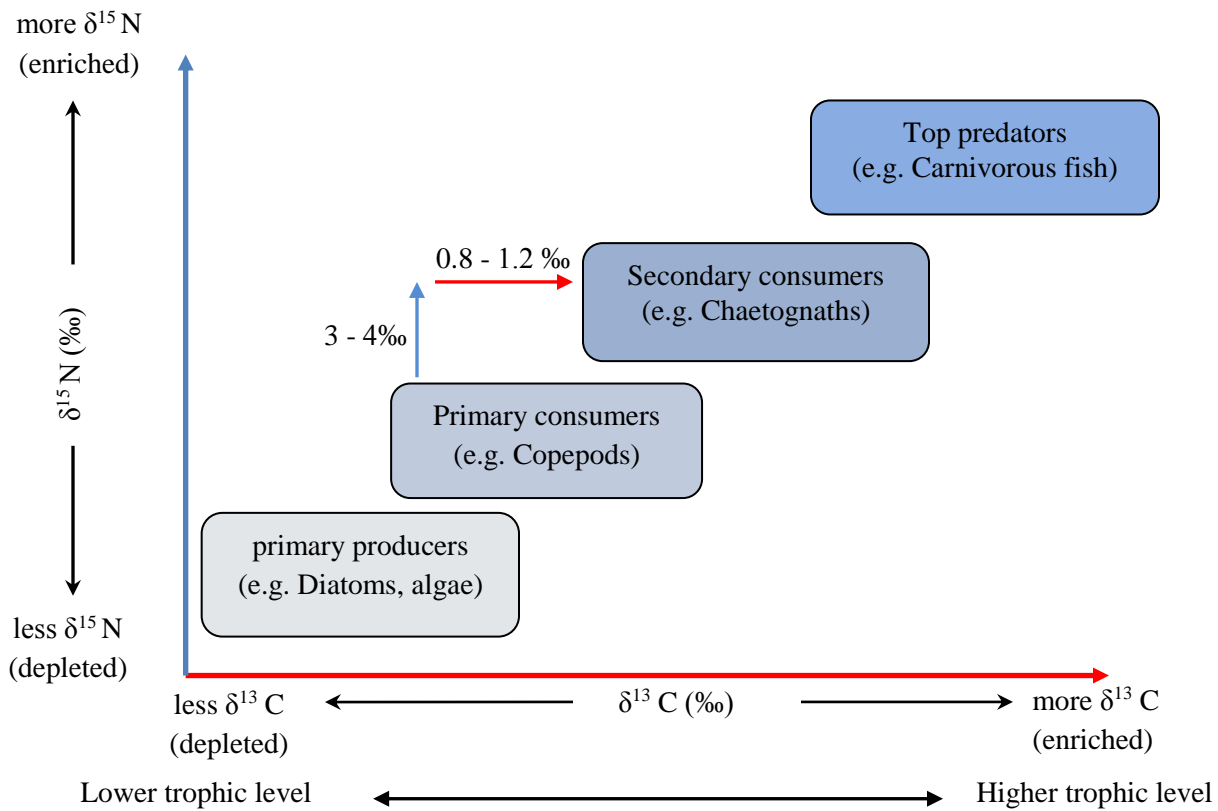
Figure 1 Conceptual model of trophic enrichment of nitrogen (δ^{15}N) and carbon (δ^{13}C) stable isotopes along trophic level in the marine food web (Muñoz, 2007, pp. 3),. Generally it assumes that in average δ^{15}N signature become enriched by 3.4‰ and δ^{13}C by 1 ‰ per trophic level.

Since year 2006, a new approach to estimates trophic positions of mesozooplankton communities were developed based on biomass size - spectra. The analysis of the distribution of biomass by size is an ataxonomic approach to study the structure and function of the pelagic ecosystem (Platt, 1985; Quinones, 1994; Rodriguez, 1994). In this approach, every individual in the system is assigned to one of a series of size-classes. The high degree of aggregation of such an approach greatly reduces the complexity of the system to a manageable level. Theories of the biomass size spectrum based on early observations made by Sheldon et al. (1972) during their research on particle size distribution of the Atlantic and Pacific Oceans. Sheldon et al. (1972) have shown that the biomass distribution of plankton organisms assumes a characteristic and predictable shape and usually show a regular decline in average biomass as the average size of organisms

increases (Figure 2). These observations led to the development of several theoretical models attempting to explain and quantify these biomass changes (Platt and Denman, 1978; Heath, 1995; Zhou and Huntly , 1997).
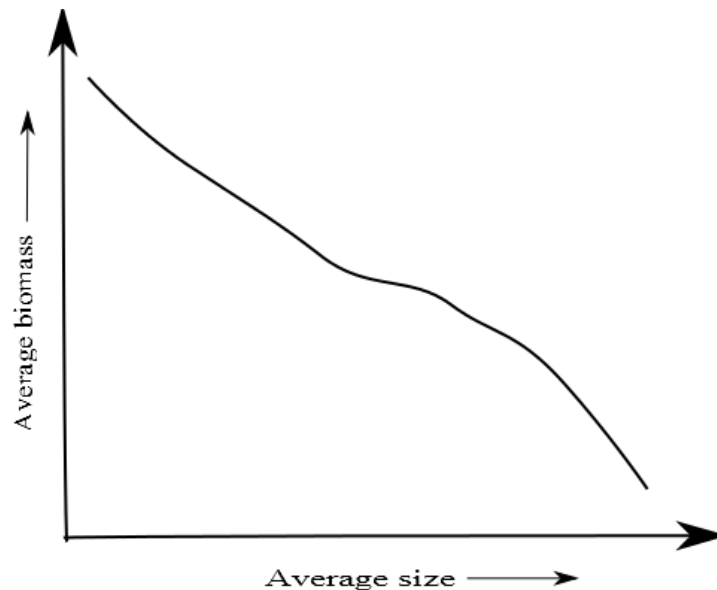
Figure 2: A regular decline in average biomass as the average size of organisms increases

Energy fluxes through aquatic systems determine the shape of the biomass spectrum (Silvert and Platt, 1978; Zhou and Huntley, 1997; Zhou, 2006). Platt and Denman (1977, 1978) explained energy flux through a given size interval as functions of individual growth within the size interval and respiration losses to the system. In contrast, Heath (1995) described the flow of energy through a group of individuals within a given size interval (cohort of individuals) as a equilibrium between population growth and mortality. Zhou and Huntley (1997) incorporated both Platt and Denman (1977, 1978) and Heath (1995) models to developed a mathematical theory of population dynamics in the context of the abundance and biomass spectra of plankton. Zhou and Huntley (1997) model described the energy flow through the biomass spectrum based on the distribution function of abundance and the law of the conservation of mass. Furthermore, the biomass spectrum theory developed by Zhou and Huntly (1997) includes all sinks (e.g. net

5

mortality including birth, depth and predation) and sources (e.g. energy from primary producers, microbial loops and population growth) which contribute to the flow of biomass through a given size interval. In addition, Zhou (2006) developed mathematical theory to compute trophic position of plankton communities based on slope of the biomass spectrum and community assimilation efficiency. These biomass spectrum theories now being progressively use to understand community processes within mesozooplankton (i.e. growth and mortality, size and taxonomic relationships, population and trophic dynamics) based on semi-automatic sampling (Basedow et al., 2010).

The intercept of the biomass spectrum represents the abundance of plankton (Zhou, 2006), thus high community abundance such as productive systems are characterized by a high intercept of the spectrum (Basedow et al., 2010). Increase of small herbivorous zooplankton with the increase of primary production leads to an accumulation of biomass at base of the biomass spectrum (small sizes), hence yield a high intercept (Zhou, 2006). In a time-dependent system, accumulated biomass at small sizes can be propagate along the biomass spectrum due to mesozooplankton cohorts development (Basedow et al., 2010). These developing mesozooplankton cohorts propagating as waves along the spectrum (Silvert and Platt, 1978; Zhou and Huntley, 1997). Slope of the biomass spectrum and community assimilation efficiency provide information on internal recycling of the biomass in mesozooplankton community, e.g. A flat slope of the spectrum indicates more internal recycling of the biomass (Zhou, 2006). Trophic positions compute based on biomass spectrum theory can have relatively high values, because all energy fluxes are taken into account. The theory has being practically used in several mesozooplankton community studies and yields reasonable values for TPs (Basedow et al, 2010). However, estimating TPs based on biovolume spectrum theory has not been extensively tested using direct sampling techniques such as stable isotope analysis.

This study focus on the trophic dynamics of zooplankton communities in different geographical areas in the North Atlantic Ocean including Iceland Basin, Reykjanes Ridge, Irminger Basin and Labrador Sea, estimated by two distinct methods; biovolume spectrum theory (BST) and stable isotope analysis (SIA). The North Atlantic is the most sampled and studied ocean of all oceans (Marra, 1995). Many oceanographic paradigms originate here, such as oceanic seasonality, ocean currents (Gulf stream, Labrador current, North Atlantic drift) and circulation in the abyss. These physical phenomena strongly affect biological processes of the region. The North Atlantic is also noted for a strong seasonal cycle in the productivity (Ho and Marra, 1994). Convective mixing in winter resets the seasonal production cycle. In springtime, the combined effects of longer, warmer days and reduced wind speeds lead to formation of a thermally stratified surface layer (Henson et al., 2006), thus induces initiating of productivity in the region. Zooplankton communities in the North Atlantic providing a crucial trophic link between the microplankton and commercially important fish stocks (Kane 1984), hence it is important have a better understand of trophic relationships of these vital marine organisms.

Therefore, here we present results from cruise conducted in the North Atlantic during March and April 2013, designed to (i) compare trophic positions estimated by biomass spectrum theory and stable isotopes analysis and (ii) identify the different trophic positions of mesozooplankton in relation to the states of the phytoplankton bloom and different water masses.

2. METHOD

2.1 Study area

The annual primary production of the North Atlantic basin has being estimated about 10.5 Gt C y^{-1} (Sathyendranath et al., 1995) and much of the export production occurs during the spring bloom (Falkowski et al., 2000). The topography of the North Atlantic includes several basins separated by sills and ridges. The Labrador Sea is the coldest and freshest basin of the North

Atlantic Ocean and the source of the intermediate depth water mass - Labrador Sea water (LSW), which may spreads throughout the entire North Atlantic (Yashayaev and Loder, 2009). The Reykjanes Ridge is the part of the Mid-Atlantic Ridge extending from Iceland to the southwest of the North Atlantic (Malmberg, 2004), which separates Iceland Basin and Irminger Basin. The Iceland Basin and the Irminger Basin are the northernmost regions of the North Atlantic Ocean (Malmberg, 2004).
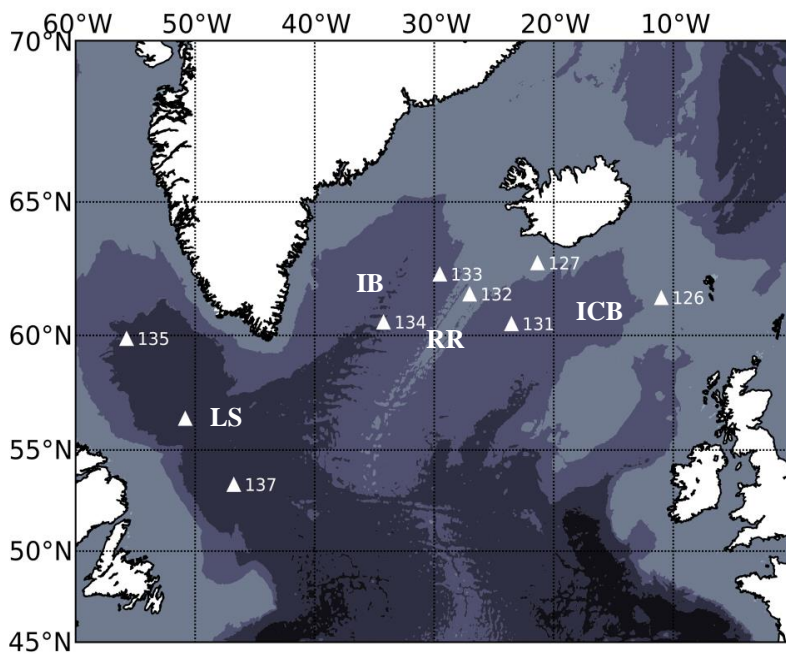
Figure 3: Map of the study area, showing the sampling stations over the Iceland Basin (ICB), Reykjanes Ridge (RR), Iminger Basin (IB), and Labrador Sea (LS).

2.2 Field sampling

Data presented in this study were collected from an area of the subpolar North Atlantic (from 61° 30 N, 11° 00W to 59° 55N, 55° 58W, Fig. 3) which was visited during the transatlantic cruise MSM 26 from Cork (Ireland) to St John's (Canada) in 2013 (20 March - 16 April). Cruise MSM 26 was part of the International EURO-BASIN project, which focused on broad scale investigation of the North Atlantic pelagic ecosystem including physical, biogeochemical and biological processes in different habitats.

The cruise covered a transect across the subpolar North Atlantic with a total of 12 stations in the Iceland Basin, Reykjanes Ridge, Irminger Basin and Labrador Sea. Hydrographical and biological data were taken from 9 stations using a platform equipped with Laser Optical Plankton Counter (LOPC; Brooke-Ocean Technology Ltd, Canada), Conductivity temperature depth sensor (CTD; Seabird 19plusV2, Seabird Electronics Inc., USA) and Fluorescence sensor (F, WetLabs EcoFl, Seabird Electronics Inc., USA). The sensors provided data including hydrography (CTD), fluorescence (F) and zooplankton abundance in the size range between 0.1 and 30 mm (LOPC). The platform was hauled vertically at a speed of 0.8 to 1.0 ms^{-2} from surface to bottom, however sampling depth was limited to 2000 m, when the depth of the sampling station exceeds the 2000 m. Data were logged every 0.5 seconds. A shipboard global position system (GPS) provided the geo-position data, which were later combined to the LOPC data. In addition zooplankton net samples were collected in the surface layer (0 - 200 m) at 7 stations for stable isotope analyses. Microzooplankton was collected by 55 μm net (MultiNet®, Hydro-Bios, Kiel, Germany) with 0.25 m^2 mouth opening. Meso and macrozooplankton were collected by 150 μm net (WP2, Hydro-Bios, Kiel, Germany) with 0.26 m^2 mouth opening. For both nets, heaving speed of the winch was between 0.2 ms^{-1} to 0.3 ms^{-1}.

This study presents bio-physical data gathered from these 7 stations including both semi automated (LOPC-CTD-F data) and zooplankton net samples (Table 1). In order to compare and interpret sized - based estimates of trophic indices computed by both biovolume spectrum theory and stable isotope analyses, data collected from the semi automated (LOPC-CTD-F data) sampling were confined to the upper 200 m.

2.3 Hydrographical and fluorescence data analyses

At each station, mean temperature and salinity values of the surface layer (0 - 200 m) were computed based on CTD profiles. Different water masses of the study area were defined by comparing observed hydrographical data with literature (e.g. Talley and McCartney, 1982; Swift, 1986; Yashayaev and Greenan, 2011).

At each station, mean chl *a* value of the upper 200 m was estimated based on fluorescence measurements. During the cruise the fluorescence sensor was calibrated against chl *a* values obtained from water samples of randomly selected sampling station. At the station, water samples from several depths (5, 15, 30, 45, 60, 75 and 100 m) within the upper 200 m were collected from corresponding 5L - Niskin bottles. Samples were filtered through GF/C filters. The remaining water from the Niskin bottles were used for measurements by the fluorescence sensor. Ashore, chl *a* values were analysed fluorometrically at the laboratory in University of Hamburg, Germany. Corresponding chl *a* values then plotted against fluorescence measured by the fluorescence sensor and a best fitted regression line for the data was drawn by using the least squares method. All fluorescence measurements (F) were converted into chl *a* values using resulting regression equation ($r^2 = 0.60$) of,

$$Chl\ a = 0.3516 \times F - 0.7055 \ (mg\ m^{-3}) .... (1)$$

Table 1: Stations in the study area - the subpolar North Atlantic Ocean, where the multinet (MN), WP 2 net and LOPC were deployed in March-April, 2013

Station	LOPC sampling				Closest net sampling						Region
	Latitude (°N)	Longitude (°W)	Date	Time (UTC)	Net type	Latitude (°N)	Longitude (°W)	Date	Time (UTC)		
126	61° 30.00'	11° 00.01'	25-Mar	01:05	MN	61° 26.91'	10° 51.77'	25-Mar	20:12		Iceland Basin
					WP 2	61° 30.00'	11° 00.01	25-Mar	04:53		
127	62° 49.28'	21° 21.74'	28-Mar	06:49	MN *	60º 31. 46´	23º 44. 88´	30-Mar	16.06		Iceland Basin
					WP 2	62° 49.28'	21° 21.73'	28-Mar	05:19		
132	61° 38.26'	27° 02.08'	01-Apr	02:07	MN	61° 38.26'	27° 02.09'	01-Apr	07:57		Reykjanes Ridge
					WP 2	61° 38.26'	27° 02.09'	01-Apr	08:30		
133	62° 24.01'	29° 31.81'	02-Apr	09:37	MN	62° 24.02'	29° 31.78'	03-Apr	02:23		Irminger Basin North
					WP 2	62° 24.05'	29° 31.74'	03-Apr	02:51		
134	60° 32.40'	34° 18.62'	05-Apr	00:25	MN	60° 32.40'	34° 18.61'	04-Apr	14:05		Irminger Basin South
					WP 2	60° 32.40'	34° 18.61'	04-Apr	13:17		
135	59° 55.66'	55° 58.78'	09-Apr	00:45	MN	59° 53.28'	55° 50.94'	08-Apr	15:03		Labrador Sea
					WP 2	59° 53.28'	55° 50.94'	08-Apr	14:24		
137	53° 21.47'	46° 45.91'	13-Apr	09:42	MN	53° 21.50'	46° 45.97'	13-Apr	08:20		Labrador Sea
					WP 2	53° 21.48'	46° 45.91'	13-Apr	08:51		

MN * - multinet sample was unable to collected from station 127, instead I used multinet sample collected from station 131 (see the map), which has similar hydrographic characteristics. At station 131, only multinet sample was collected and WP 2 sample was unable to obtained due to net damage. Therefore $\delta^{15}N$ value of microzooplankton collected from multinet at station 131 was used as a reference base line to determine trophic positions of meso and macrozooplankton collected by the WP 2 net at station 127.

2.4 LOPC data analyses

2.4.1 LOPC data processing

The LOPC is the second generation of optical plankton counter providing continuous real-time information on the size and abundance of particles in the water (Herman, 1988, 1992; Herman et al., 1993), and also information on the morphology of zooplankton (Herman et al., 2004). When the instrument is hauled through the water, zooplankton and other particles pass through a laser beam (1 mm in width) inside the instrument and their number, size and transparency is registered on a matrix of photo diodes. The LOPC uses 35 photodiodes to detect the transparency of each particle passing through the laser sheet of light in the sampling tunnel. LOPC discriminate counted particles in to two types depending on the number of neighboring subunits of the detector are activated by the passing particle. A particle covering all or part of one or two subunits is called a single-element particle (SEP) and a particle that span at least three or more subunits is called a multi-element particle (MEP). The size of particles is registered as a digital size, which can be converted into equivalent spherical diameter (ESD), i.e. the diameter of a sphere with an volume corresponding to the volume estimated for the particle passing through the LOPC. SEPs are automatically registered into 1 of 122 ESD size categories between 0.09 and 1.92 mm ESD. MEPs, typically > 0.8 mm ESD (Basedow et al., 2013) are recorded along with the information on their shape and are converted to ESD using a function provided by the manufacturer. The instrument can detect particles within a range of 0.1–30 mm equivalent spherical diameter (ESD). Particles counted by the LOPC were grouped into 50 size groups of equal body volume increments to increase statistics and to simplify data presentation.

All LOPC data were processed and analysed using the python (version 3.3.4) and R (version 3.0.2) programming languages.

2.4.2 Biovolume spectra

Biovolume spectra can be used, replacing the biomass spectra if relation between body size and biomass is unknown (Zhou, 2006). Biovolume spectrum is unique for a given plankton community (Zhou et al., 2010) and shape of the spectrum is determine by energy fluxes through the plankton community (Platt and Denman, 1978; Zhou and Huntley,1997; Zhou, 2006). A normalised biovolume spectrum *b* is defined as (Edvardsen et al., 2002; Quinones et al., 2003),

$$Biovolume\ spectrum\ (b) = \frac{biovolume\ in\ size\ interval\ \Delta w}{size\ interval\ \Delta w}\ (in\ m^{-3}).............................(2)$$

where, w is the body volume of a zooplankter in mm^3.

To compare biovolume spectrum in different regions, the slope of a biovolume spectrum on logarithmic coordinates was computed for the whole zooplankton community (S to L, see section 2.6) by using the least-squares fit of a linear function.

2.5 Stable-isotope analyses

2.5.1 Sample preparation

Upon recovery, retained zooplankton were wash off the nets into jars. At each station, each net sample was split into 200 and 50 ml fractions and 200 ml fraction of the sample was prepared for stable isotope analysis (see section 2.5.1a and 1b); the remaining plankton sample was preserved in a 40% formaldehyde–seawater solution for taxonomic analysis (not presented in this paper).

2.5.1a Microzoopankton

At each station, in the shipboard laboratory, the content of the collecting flask of the multinet was first transferred into a jar and its level was brought up to 250 ml by adding filtered sea water (FSW - was prepared by filtering sea surface water through the 40 μm sieve). Suspended particles (plankton) were collected by gentle vacuum filtration of 200 ml of the sample through a 47 mm pre-weighted GFA filter. The filter with particles was then dried at 55 ºC for 24 hours and stored for analysis ashore.

2.5.1b Meso and macrozooplankton

At each station, the content of the collecting flask was first transferred into a jar and its level was brought up to 250 ml by adding FSW. 200 ml of the sample was subsequently fractionated through sieves of 2.0, 1.0, 0.5 and 0.2 mm and each fraction was carefully washed with FSW and transferred to 47 mm pre-weighted GFA filter papers. Samples were dried at 55 ºC for 24 hours and stored until further analysis.

2.5.1c Blank

A blank filter was prepared at each sampling station to characterize background nitrogen value of surrounding water by pre-filtering 250 ml of surface sea water through a 40 μm sieve and subsequently filtering through the pre-weighted GFA filter. The filter was dried and stored with the corresponding plankton samples.

2.5.2 Stable isotope determination

Stable isotope analyses were carried out at Centro Oceanográfico de A Coruña, Instituto Español de Oceanografía, Spain. Natural abundance of nitrogen isotope were measured using an isotope-

ratio mass spectrometer (Finnigan Matt Delta Plus) coupled to an elemental analyser (Carlo Erba CHNSO 1108). Nitrogen stable isotope abundance was expressed as δ^{15}N in parts per thousand (‰) relative to atmospheric N_2 isotope standards.

$$\delta^{15}N = \left(\left(R_{sample}/R_{standard}\right) - 1\right) \times 1000 \dots\dots\dots\dots\dots\dots(3)$$

where, R is the ratio of ^{15}N/^{14}N.

2.6 Zooplankton composition and size classification

The level of taxonomic identification was not covered in this study. Instead literary records of common zooplankton species/groups in the study area, their ESD sizes and prosome lengths were used to develop common size classification for particles, based on data from the LOPC and the size fractionated net samples (Table 2). Based on the results, particles were divided into 3 size classes: small (S), medium (M) and large (L) (Table 3). However, determining the size range will always be somewhat subjective and most of the time zooplankton species/groups can overlap each other. Particles from 0.10 - 0.25 mm ESD and from the 0.055 - 0.2 mm size fraction were not included in the analyses, because such small particles may result from eroded phytoplankton aggregates and other detrital particles. Particles with an ESD > 4 mm were excluded from the analyses as few particles were registered by the LOPC in this size range at most of the sampling stations. In addition, *Calanus finmarchicus* was the dominant zooplankton species observed in all sampling stations during the study period (own observation), therefore ESD and prosome length of the different development stages (*Calanus* spp. nauplii to CVI female) in the size classification are relevant to the *C. finmarchicus.*

Table 2: Common zooplankton species/groups in the North Atlantic Ocean, their ESD sizes and prosome lengths data recorded in early studies. Based on the results zooplankton counted by the LOPC and size fractionated net samples were classified as small (s), medium (M) and large (L) size classes.

Species/groups	ESD (mm)	Prosome length (mm)	Size class
Calanus spp. [a b c d f p]			
- Nauplii	~0.25 - 0.6[a b]	0.2 - 0.6[a d]	S
- CI	0.5[c]	< 1.0[c g]	S
- CII - CIII	~0.6 - 1.0[c e]	~1.0- 1.5[c g]	M
- CIV - CVI females	~1.1 - 2.0[c e]	~2.0 - 2.6[c]	L
Metridia spp.[a d k]	~0.3 - 1.0[a]	0.55 - 1.8[g i]	S and M
Microcalanus spp. [a d k n j]	< 0.6 [d]	~0.6 - 1.1[e]	S
Pseudocalanus spp. [a d k n]	~0.3 - 1.0[b d]	~0.2 - 1.2[f g i]	S and M
Oithona spp. [c d e n k]	~0.3 - 0.5[b d]	~0.1 - 1.0[f i]	S
Euphausids [d m n h k]	> 1.8[b]	> 2.0[g]	L
Chaetognaths [d o k]	~1.1 - 1.5[b]	> 2.0[b g]	M and L
Balanus nauplii [o]	~0.25 - 0.6[b]	~0.75 (mean)[h]	S
Hydrozoa [i]	0.25 - 0.95[b]	0.77 ± 0.42[b]	S and M
Oncaea spp. [o k]	< 0.5[d]	~ 0.3 - 0.8[i]	S

(1st column: a:Beaugrand et al., 2002; b:Planque and Taylor, 1998; c:Castellani et al., 2008; d:Krause et al., 2003; e :Gallienne and Robins, 2001; f:Fry and Quinones, 1994; g:Unstad and Tande, 1991; h:Cleary et al., 2012; i:Gibbon and Richardson, 2009; j:Walter, T.C., and Boxshell, G., 2014; k:Head et al., 2003; l:Johns et al., 2001; m:Letessier et al., 2011; n:Gislason, 2003; o:Barnard et al., 2004)

(2nd column: a:Zhou et al., 2009; b:Basedow et al., 2010; c:Edvardsen et al., 2002; d:Forest et al., 2012; e:Basedow et al., 2006)

(3rd column: a:Ogilvie, 1953; b:Basedow et al., 2010; c:Edvardsen et al., 2002; d:Prokopchuk, 2003; e :Zooplankton Identification Manual for North European Seas, 2014; f:Cohen and Lough, 1981; g:Piontkovski and Melnik, 2008; h:Turner et al.: 2001; i:Conway, 2012)

Table 3: Classification of size classes applied to the LOPC and size fractionated net samples data. Zooplankton was divided into 3 classes: small (S), medium (M) and large (L). Zooplankton species/groups within each size class were determined based on literature values, see Table 2.

Size class	ESD (mm)	Size fraction (mm)	Common zooplankton species/groups
S	0.25 - 0.6	0.2 - 1.0[a]	*Calanus* spp. nauplii, *Oithona* sp., *Microcalanus* spp., *Pseudocalanus* spp., Hydrozoa, Balanus nauplii, *Metridia* spp., *Oncaea* spp. *Calanus* spp. CI
M	0.6 - 1.0	1.0 - 2.0	*Pseudocalanus* spp., *Calanus* spp. CI I- CIII, *Metridia* spp., Hydrozoa Chaetognaths
L	1.0 - 4.0	> 2.0[b]	*Calanus* spp. CIV - CVI, Chaetognaths, euphausids

[a] Size fractions of 0.2 - 0.5 and 0.5 - 1.0 were grouped to have S size class.

[b] Size fraction > 2.0 mm (L class) refers to the size range from 2.0 mm to size fraction corresponding to 4 mm ESD.

2.7 Zooplankton abundances

Average zooplankton abundance in the upper 200 m were estimated for all stations and all size classes (S,M and L) based on abundance data recorded by the LOPC.

2.8 TPs estimation

Trophic positions of the zooplankton, which were assumed to be representative of primary consumers such as herbivorous copepods to top consumers such as chaetognaths were investigated through the biovolume spectrum analyses and use of nitrogen stable isotope tracers.

2.8.1 TPs estimation from biovolume Spectrum analyses

Biovolume spectra were constructed for all 7 stations and from each biovolume spectrum, one slope was calculated for the entire size range (S to L) and three separate slopes for each of the size ranges of the three zooplankton groups (S, M and L). To assess the community structures associated with trophic dynamics, the trophic positions for each group (S, M and L) and for the

17

whole zooplankton community (S to L) were estimated based on the slopes of biovolume spectra

(b) and the mean assimilation efficiency of zooplankton (μ_n) (Zhou, 2006).

$$TP = \frac{-(1+\mu_n)}{(\delta \ln b / \delta \ln w)} \quad \text{............................ (4)}$$

The computation of TPs is based on the assumption that the biovolume spectrum can be

linearized on a logarithmic scale (Zhou, 2006). Therefore, at first data were checked for the

linearity and found consistent with the assumption. Furthermore, to compute TPs, the

assimilation efficiency of the zooplankton community has to be known (Zhou, 2006). I have used

a mean assimilation efficiency of 70%, a value typically used for copepods (Basedow et al.,

2010). However the existing data of zooplankton assimilation efficiency shows a greater

variability depending on food source, species, body weight, temperature and development stage

(Mauchline, 1998; Almeda et al., 2011) . For instance, assimilation efficiency of *Oithona*

davisae ranges from 65% to 86% depending on body weight, temperature and development stage

(Almeda et al., 2011). For carnivores zooplankton, assimilation efficiency may be as high as

98% (Mauchline, 1998). Therefore, TPs estimates that are made choosing of constant

assimilation efficiency for all size classes and species/groups may not represent exact TPs, but

the variations of TPs represent the trophic dynamics of plankton communities.

2.8.2 TPs estimation from stable isotope analyses

Mesozooplankton trophic positions for each size fraction (0.2 - 0.5, 0.5 - 1.0, 1.0 - 2.0 and > 2.0)

were calculated based on the assumption that $\delta^{15}N$ signature becomes enriched by 3.4‰ per

trophic level, and that the 0.055 - 0.2 mm size fraction acts as the reference baseline with a

trophic level of 1.5 (mixture of phytoplankton and primary consumers). The 0.055 - 0.2 mm size

fraction obtained from the station 131 was used as reference baseline for station 127 (see Table 1). The trophic positions of each mesozooplankton size fraction i (TPi) was calculated as:

$$TPi = (\varDelta\ \delta^{15}Ni\ /3.4) + d............................(5)$$

where, d is 1.5.

2.9 Comparison of TPs

TPs estimated from the LOPC data were compared with those estimated from the δ^{15} N stable isotope analyses. In order to make common size classification (section 2.6) TP of 0.2 - 0.5 and 0.5 - 1.0 sized fractions estimated by stable isotope analyses were grouped and a mean value was assigned for TP of 0.2 - 1.0 size fraction (S size class). For the comparison, TPs estimated by both methods and δ^{15} N variations were plotted in the same graph against the sampling stations. Moreover, predictions have been made by previous studies (Basedow et al., 2010; Zhou, 2006) for biovolume spectrum to yield relatively higher TPs than direct sampling methods which was confirmed by this study. Therefore, a Mean Trophic Position Increment (MTPI) was introduced to determine deviation factor of TPs between the two methods,

$$Mean\ Trophic\ Position\ Increment\ (MTPI) = \frac{MTP_{(Biovolume\ spectrum\ analyses)}}{MTP_{(Stable\ isotope\ analyses)}}$$

$$Mean\ Trophic\ Position\ (MTP) = \frac{(TP_1+TP_2+\cdots+TP_n)}{n}$$

where n is number of TP. MTPI was calculated for the each size class and for the whole zooplankton community, except for the medium size class due to the unavailability of TPs estimates for biovolume spectrum analyses. Finally, based on observed MTPI and slopes of the biovolume spectra, a hypothetical model was developed to interpret possible reasons for the deviations.

3. RESULTS

3.1 Hydrograpy and fluorescence

In general, along the transatlantic transect, there was a marked longitudinal gradient in the mean salinity and temperature recorded by the CTD. At the eastern end of the cruise track, the salinity and temperature ranged between 35.2 - 35.3 and 7.8 - 8.7 °C respectively, while further to the west salinity and temperature decreased to a range of 34.5 - 34.7 and 3.8 - 4.6 °C respectively (Fig. 4). Two distinct water masses were identified by tracking salinity and temperature variations along the transect; warm, saline Atlantic water (AtW, salinity > 35.0 and temperature > 0 °C, Swift, 1986) and cold, less saline Labrador Sea surface water (LSSW, salinity < 34.97, Yashayaev and Greenan, 2011). Surface water of stations over the Iceland Basin, Reykjanes Ridge and northern-most part of the Irminger Basin were dominated by warmer AtW. LSSW were found at stations in the Labrador Sea and southern-most part of the Irminger Basin, where, Labrador Sea water advecting into the Irminger Sea (Tally and McCartney, 1982). Weakly developed stratified layer can be observed within upper 50 - 80 m in the Labrador Sea, while the water columns over the Iceland Basin, Reykjanes Ridge and Irminger Basin appeared to be well mixed approximately down to the 500 m (CTD profiles, only the upper 200 m are shown, Fig. 5).

The chl a concentration remained very low (0.07 - 0.21 mg chl a m^{-3}) along the transect during the cruise and was not linked to water mass characteristics (Fig. 4). Minimum chl a concentrations were observed at eastern (station 126) and western (station 135) ends of the transect (0.07 mg chl a m^{-3} per each) . Fairly high chl a concentration was observed at station 137 in the Labrador Sea with a maximum value of 0.21 mg chl a m^{-3}, followed by the chl a concentration of station 132 over the Reykjanes Ridge (0.17 mg chl a m^{-3}). Relatively a moderate chl a concentrations were observed in stations over the Irminger Basin (0.14 mg chl a m^{-3} per each).
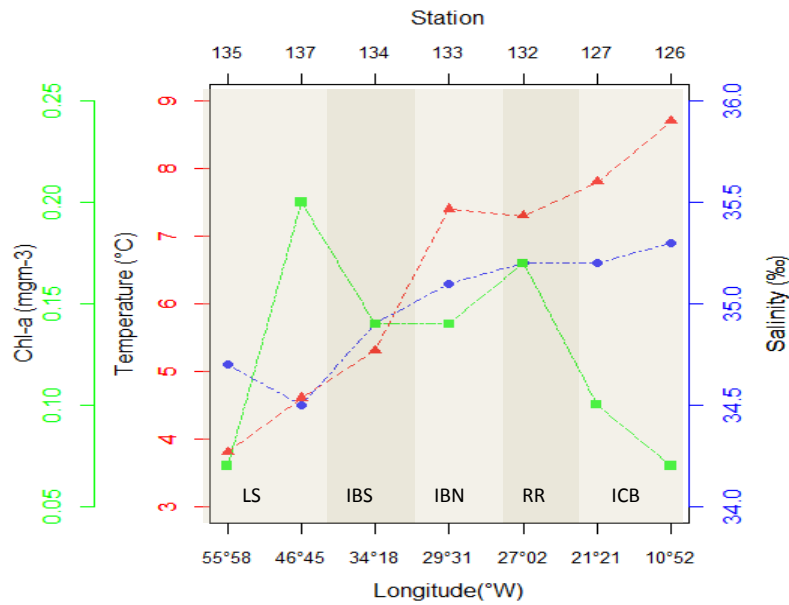
Figure 4: Mean salinity, temperature and chl *a* variations along the transatlantic transect from east (right) to west (left). There was a marked longitudinal gradient in the mean salinity and temperature. Chl *a* distribution was not linked to water mass characteristics and did not show any longitudinal gradient.

ICB - Iceland Basin

RR - Reykjanes Ridge

IBN - Irminger Basin North

IBS - Irminger Basin South

LS - Labrador Sea
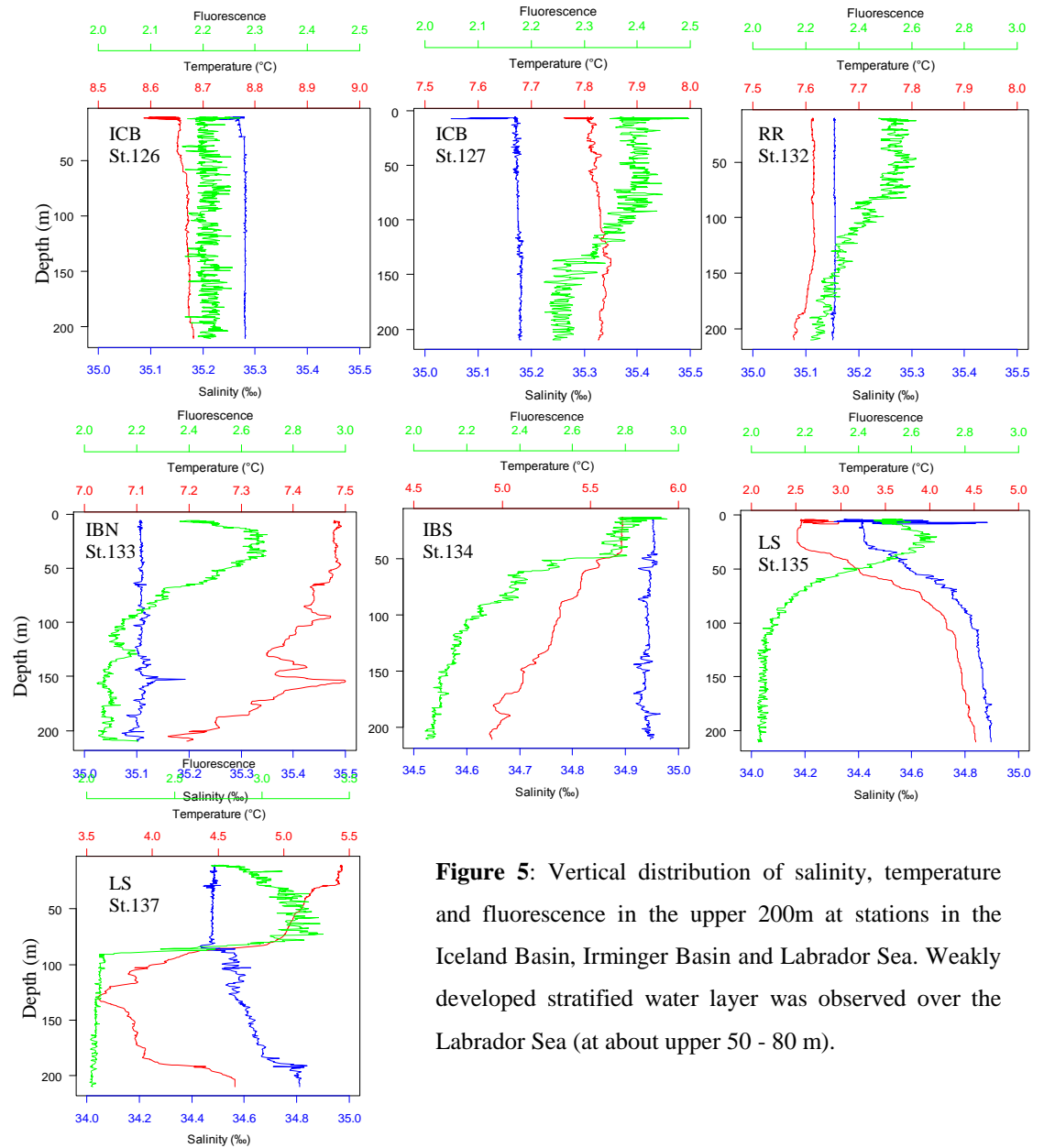
Figure 5: Vertical distribution of salinity, temperature and fluorescence in the upper 200m at stations in the Iceland Basin, Irminger Basin and Labrador Sea. Weakly developed stratified water layer was observed over the Labrador Sea (at about upper 50 - 80 m).

3.2 Zooplankton abundances

There was a non-uniform distribution of zooplankton abundance across the transatlantic transect. Zooplankton abundance was corresponded roughly to the pattern in chl *a*. Total mesozooplankton abundance was lower in the Iceland Basin and Reykjanes ridge (average of 372 and 352 ind m^{-3} respectively), whereas those in the Irminger Basin and Labrador Sea were relatively high (average of 1157 and 2884 ind m^{-3} respectively) (Fig. 6). The highest zooplankton abundance was recorded at the station 137 in Labrador Sea with a maximum value of 4457 ind m^{-3}, where the maximum chl *a* concentration was observed. Densities of the medium and large-sized zooplankton were approximately in order of magnitude lower than the small-sized zooplankton in most of the hydrographic regions.
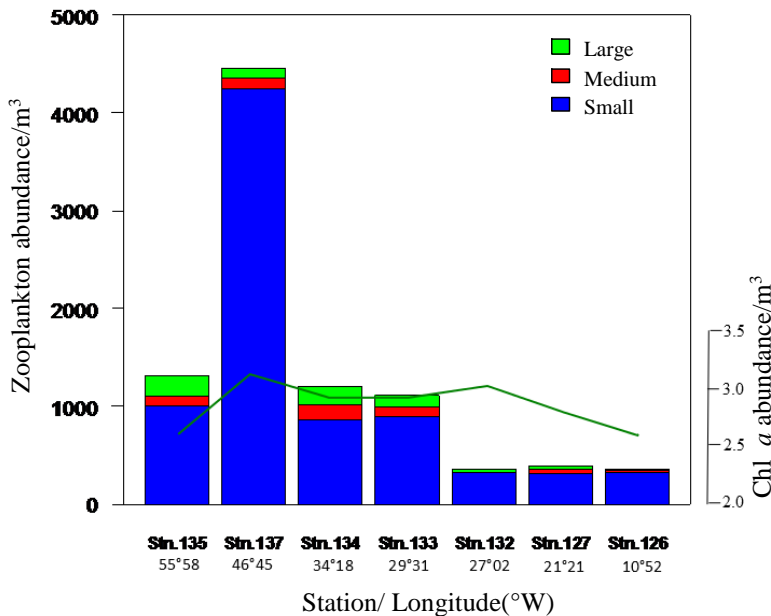
Figure 6: Abundance distribution of the small, medium and large-sized zooplankton along the transatlantic transect in relation to the chl *a* variation (green line) in March - April 2013.

3.3 Biovolume Spectra

Collecting data into logarithmically equal biovolume size categories indicated an almost consistent decrease in total zooplankton biovolume with increased size in all stations (Fig. 7). In general, biovolume spectra yielded low intercepts for the all stations and ranged between 0.82
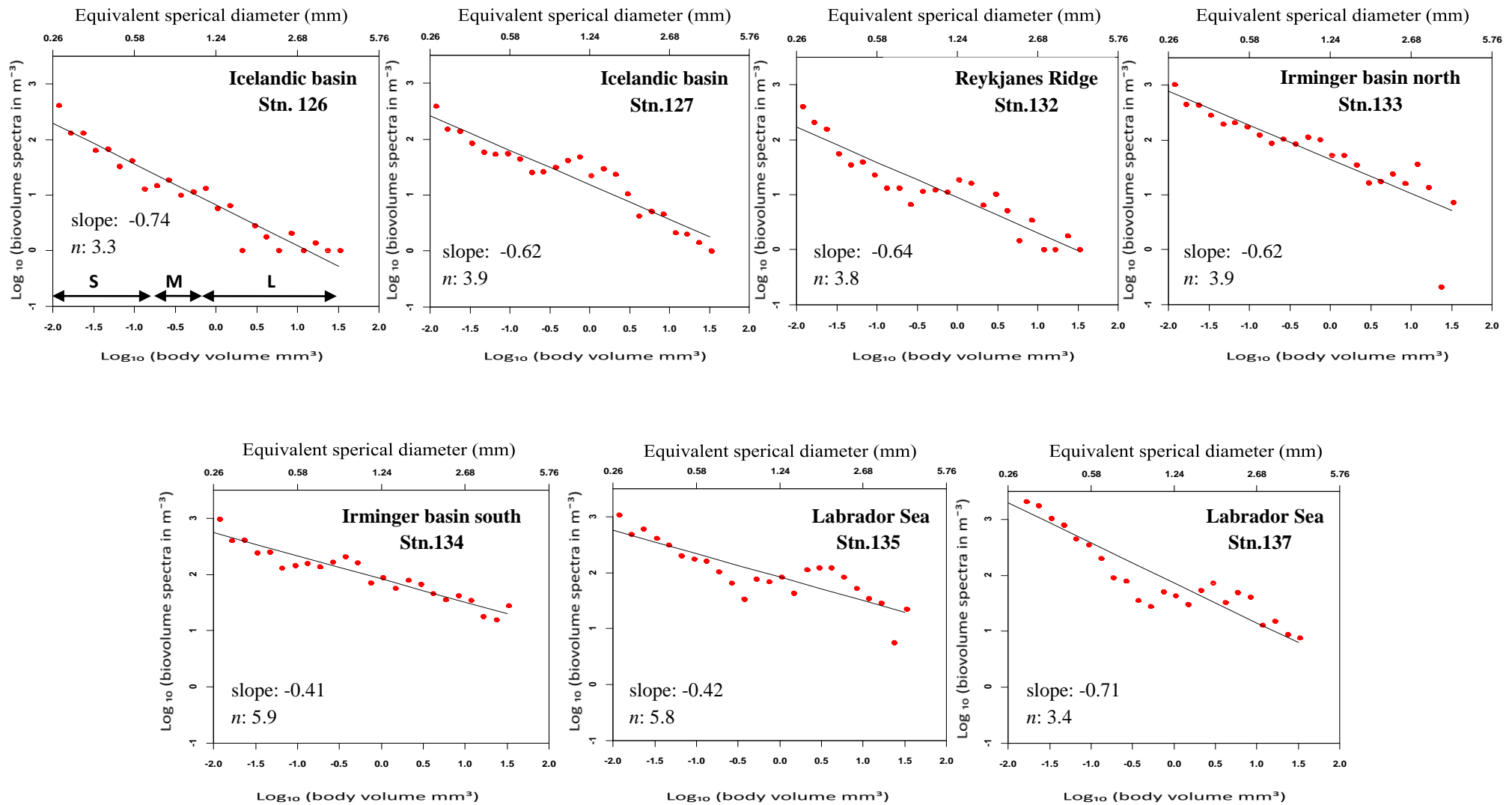
Figure 7: Biovolume spectra of the zooplankton community in March-April 2013 at the stations; Iceland Basin, Irminger Basin and Labrador Sea, associated slope and predicted numbers of internal biomass recycles (assuming the community assimilation efficiency of 70%.)

Table 4: Parameters of the linear functions fitted to the biovolume spectra, obtained from LOPC data collected at the stations along the North Atlantic transect.

Station	Region	Water mass	Size group	Slope	Intercept	r^2	P-value
126	Iceland Basin	AtW	0.25 - 0.6	-1.07	0.37	0.89	< 0.001
			0.6 - 1	-0.16	1.03	-0.40	0.7367
			1 - 4	-0.62	0.76	0.69	< 0.001
			All	-0.74	0.82	0.93	< 0.001
127	Iceland Basin	AtW	0.25 - 0.6	-0.88	0.70	0.88	< 0.001
			0.6 - 1	-0.27	1.32	-0.13	0.5063
			1 - 4	-0.98	1.48	0.95	< 0.001
			All	-0.62	1.18	0.91	< 0.001
132	Reykjanes Ridge	AtW	0.25 - 0.6	-1.27	0.01	0.93	< 0.001
			0.6 - 1	-0.34	0.81	-0.18	0.541
			1 - 4	-0.76	1.10	0.80	< 0.001
			All	-0.64	0.95	0.87	< 0.001
133	Irminger Basin North	AtW	0.25 - 0.6	-0.75	1.40	0.88	< 0.001
			0.6 - 1	-0.26	1.82	0.19	0.324
			1 - 4	-0.88	1.85	0.51	< 0.01
			All	-0.62	1.65	0.78	< 0.001
134	Irminger Basin South	AtW	0.25 - 0.6	-0.84	1.22	0.90	< 0.001
			0.6 - 1	0.29	2.41	0.38	0.2343
			1 - 4	-0.44	1.95	0.82	< 0.001
			All	-0.41	1.92	0.91	< 0.001
135	Labrador Sea	LSW	0.25 - 0.6	-0.71	1.53	0.88	< 0.001
			0.6 - 1	-1.50	0.91	0.99	< 0.01
			1 - 4	-0.43	1.98	0.39	< 0.05
			All	-0.42	1.92	0.75	< 0.001
137	Labrador Sea	LSW	0.25 - 0.6	-1.19	1.29	0.98	< 0.001
			0.6 - 1	-1.54	0.92	0.91	<0.05
			1 - 4	-0.39	1.69	0.46	< 0.01
			All	-0.71	1.87	0.86	< 0.001

and 1.92. However, the stations in the Irminger Basin and Labrador Sea had relatively high intercepts (1.65 - 1.92), than the intercepts of stations in the Iceland Basin and Reykjanes Ridge (0.82 - 1.18), reflecting the observed high zooplankton abundances in the Irminger Basin and Labrador Sea and low abundances in the Iceland Basin and Reykjanes Ridge. Relatively flatter

slopes of -0.41 and -0.42 were observed in the southern-most part of the Irminger Basin (station.

134) and northwest end of the Labrador Sea (station 135) respectively, where the Labrador Sea

surface water (LSSW) was dominated. Thus, the maintenance of such flat slopes indicating that

biomass has been recycled within the mesozooplankton community several times. In contrast

more steeper and relatively uniform slopes, ranged between -0.62 and -0.74 were observed for all

the other stations in the study area (Fig. 7, Table 4), indicating a higher loss of energy from the

mesozooplankton community.

3.4 $\delta^{15}N$ isotope

In general, all zooplankton size groups showed the same pattern of spatial variation along the

transect, although the relationship between $\delta^{15}N$ and size groups showed some variation among

stations. In addition, zooplankton showed a weak association between size and $\delta^{15}N$. Only two

stations followed by a typical relationship of increasing $\delta^{15}N$ with   animal size (stations 132

and 133), while no such consistent trend was observed in other stations. Many stations along the

transect $\delta^{15}N$ of S sized zooplankton was higher than that of M sized zooplankton (Stations 126,

127, 134, 135) and higher than that of L sized zooplankton in stations 127 and 135 (Fig 8, b).

Further, for the all size groups (S,M and L group), relatively constant $\delta^{15}N$ values were observed

in the western part of the transect extending from the northern Irminger Basin to northwest

Labrador Sea, while more fluctuations in $\delta^{15}N$ were observed in the eastern part of the transect

from the Iceland Basin to Reykjanes Ridge (Fig 8, a).

Maximum $\delta^{15}N$ for S sized zooplankton was recorded in the stations 126 & 135 (6.1 and 5.7‰

respectively). $\delta^{15}N$ enrichment was highest for M and L sized zooplankton in station 132 over

the Reykjanes Ridge (7.5 and 9.6‰, respectively) . The isotopic spread among zooplankton

size groups at a single station ranged from 0.7% to 6.7%, with generally smaller spreads in the stations over the Iceland Basin and northwest Labrador Sea.
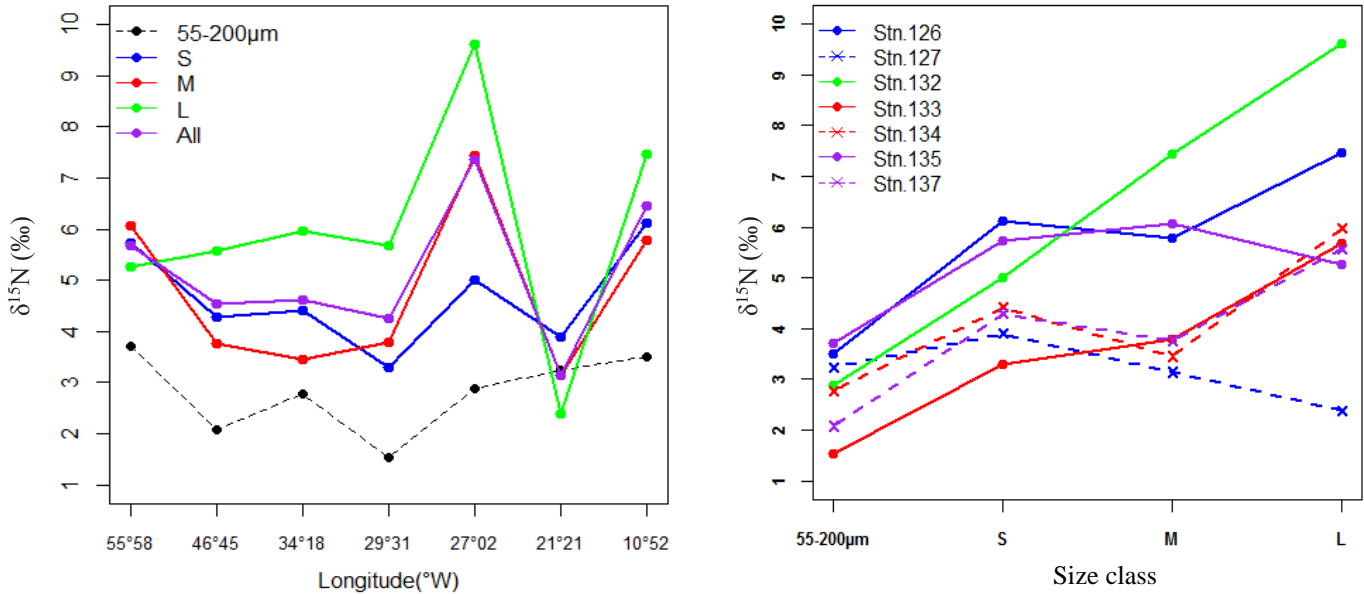
Figure 8: $\delta^{15}N$ variations of the small (S), medium (M) and large (L) sized zooplankton relation to the base line size fraction of the 55 - 200 μm, **a)** along the transatlantic transect and, **b)** at each station.

3.5 TPs variation along the transect

TPs estimated from the stable isotope analyses for small-sized zooplankton was ranged between 1.7 and 2.3; these moderate TPs may indicating that the small-sized zooplankton in the upper layer along the transect was feeding on omnivorous diet during the period of study. TPs estimated from the biovolume spectrum theory also yielded comparable, but slightly higher values than the isotopic estimations and ranging between 1.9 and 3.4 (Table 5, Fig. 9). TPs of small-sized zooplankton computed from both methods did not link to either of water mass characteristics or $\delta^{15}N$ variations along the transect. Except the Labrador Sea, no significant TPs were found for the biovolume spectra of medium-sized zooplankton to compare those with the stable isotope estimations. TPs of medium-sized zooplankton estimated from the stable isotope

analyses had relatively constant values throughout the area, ranging between 1.5 and 2.8. These moderate TPs indicating that these medium-sized zooplankton were also feed on more omnivorous diet. Moreover, the variation of TPs of medium-sized zooplankton was well consistent with the $\delta^{15}N$ variations along the transect ($p < 0.01$) (Table 6).

TPs of large-sized zooplankton estimated based on biovolume spectrum showed mark relationship with the water mass characteristics. Very high TPs were observed in western portion of the transect extending from the northern Irminger Basin to northwest Labrador Sea (5.5 - 6.3), where the LSSW was dominated. In contrast relatively moderate TPs were observed in eastern part of the transect extending from the Iceland Basin to southern Irminger Basin (2.5 - 3.9) and the dominate water mass was AtW. However, the results of biovolume spectrum theory did not significantly correlated with the $\delta^{15}N$ variations along the transect. On the other hand, TPs estimated from stable isotope for the large-sized zooplankton did not show any link to the water mass characteristics, but were significantly correlated to the $\delta^{15}N$ variations along the transect ($p < 0.001$) . TPs of whole zooplankton community estimated based on biovolume spectrum theory also had a link to the water mass characteristics of the region. Relatively uniform and moderate TPs (ranging from 3.3 to 3.9) were observed in stations where the AtW was dominated. Relatively high TPs (ranging from 5.5 to 5.7) were observed in stations where the LSSW was dominated, but with a notable exception in station 137, where the community had moderate TP (3.4). Furthermore TPs did not correlate to the $\delta^{15}N$ variations along the transect. In contrast, community trophic positions computed based on stable isotope analyses did not link to the water mass properties, but significantly correlated to the $\delta^{15}N$ variations ($p < 0.05$). Further TPs were relatively constant throughout the region, ranging between 1.5 and 2.8.

Table 5: TPs of zooplankton community estimated based on biovolume spectrum theory (BST) and stable isotope analyses (SIA) in stations along the transatlantic transect; March-April 2013. In biovolume spectrum analyses, TPs were computed from slope of the biovolume spectra for S, M, L and whole zooplankton community (all) only if slopes were significant. n.s - not significant.

	Trophic position (TP)													
Size class	126		127		132		133		134		135		137	
	BST	SIA	BST	SIA	BST	SIA	BST	SIA	BST	SIA	BST	SIA	BST	SIA
S	2.3	2.3	2.7	1.7	1.9	2.1	3.2	2.0	2.9	2.0	3.4	2.1	2.0	2.2
M	n.s.	2.2	n.s.	1.5	n.s.	2.8	n.s.	2.2	n.s.	1.7	1.6	2.2	1.6	2.0
L	3.9	2.7	2.5	1.3	3.2	3.5	2.8	2.7	5.5	2.4	5.7	2.0	6.3	2.5
All	3.3	2.4	3.9	1.5	3.8	2.8	3.9	2.4	5.9	2.0	5.8	2.1	3.4	2.2
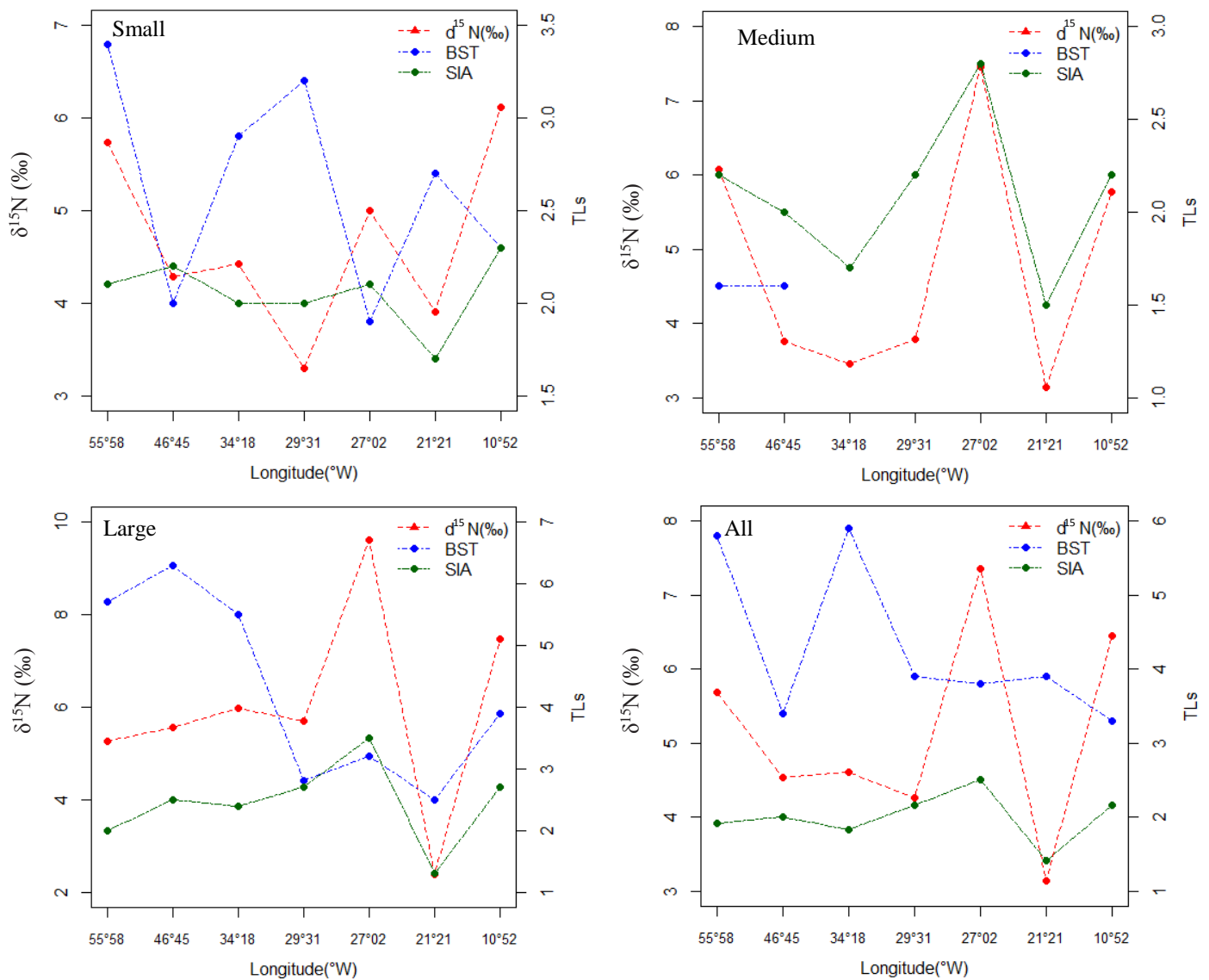
Figure 9: Variations of TPs; small, medium, large and whole zooplankton community (all), estimated from both biovolume spectrum theory (BST) and stable isotope analyses (SIA) in relation to the δ^{15}N variations of stations along the transatlantic transect.

Table 6: Correlation between TP and $\delta^{15}N$ along the transect. No significant correlation was found for small-sized class either BST or SIA. There was a significant correlation between TP estimated from SIA and $\delta^{15}N$ for medium, large and whole (All) zooplankton community.

Size class	BST		SIA	
	r	p - value	r	p - value
S	-0.1594	0.7329	0.6338	0.1264
M	-	-	0.8746	**0.0099**
L	0.0243	0.9587	0.9547	**0.0008**
All	-0.0796	0.8654	0.8242	**0.0225**

3.6 Comparison of TPs estimated from BST and SIA

In general, the TPs computed from the biovolume spectrum theory had relatively high trophic indices for small, large and whole zooplankton community than those estimated from the stable isotope analyses (Fig. 10). However TPs of small-sized zooplankton computed based on the biovolume spectra did not significantly differ from those estimated based on stable isotope analyses ($p > 0.05$). But TPs of large-sized and whole (all) zooplankton community shows significant differences between the two methods with increased significant level towards the whole zooplankton community ($p < 0.05$ and 0.01 respectively) (Table 7). Further Mean Trophic Position Increament (MTPI) increased as small < large < whole (all) zooplankton community (1.2, 1.7 and 1.9 respectively).
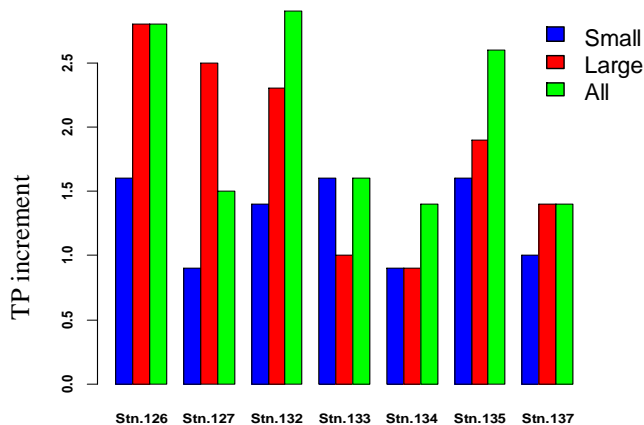
Figure 10: Increment of TPs estimated from BST relative to the TPs estimated from SIA for small, large and whole(All) zooplankton community

Table 7: Results of Wilcoxon rank sum test performed to determine whether the TPs estimated from BST was significantly different from those estimated from SIA for small, large and whole (All) zooplankton community. TP increment and p-value increasing from small to whole zooplankton community.

Size class	Mean TP BST	Mean TP SIA	MTPI BST/SIA	Wilcox.test p - value	Significant level
S	2.5	2.0	1.2	$p = 0.1079$	$p > 0.05$
M	-	-	-	-	-
L	4.3	2.5	1.7	$p = 0.0178$	$p < 0.05$
All	4.3	2.2	1.9	$p = 0.0021$	$p < 0.01$

4. DISCUSSION

The combination of TPs estimations using biovolume spectrum theory with stable isotope analyses, well resolved uncertainties of TPs estimations based on biovolume spectrum theory. The results of this study confirm that estimated TPs based on biovolume spectrum theory reliably describe the trophic relationships within the mesozooplankton community. Moreover, the study reveal that biovolume spectrum may compute relatively higher trophic indices for mesozooplankton size classes compared to direct sampling methods, e.g. stable isotope analyses, due to its ability to detect internal recycling of the biomass through microbial loop organisms. Findings of this study thus proved applying of biovolume spectrum theory to data obtained by LOPC as a high resolution method not only for estimation of TPs, but also to trace the influence of microbial processes for the sustainability of mesozooplankton communities in relation to different environmental conditions.

4.1 Hydrography and mesozooplankton abundance distribution

Hydrographical properties of the study area revealed relatively low salinity and temperature over the Labrador Sea and southern-most part of the Irminger Basin. Further, there was a stratified

water layer in the Labrador Sea, which extended down to 30 to 80 m. The Labrador Sea is the coldest Sea in the North Atlantic Ocean (Lazier et al., 2002). Also during the period of investigation observed temperatures in the Labrador Sea were lower than in the rest of the study area, but higher than those observed during winter conditions in the Labrador Sea (Yashayaev and Greenan, 2011). Thus, a major cause for the observed freshening of the surface layer and shallow mixed-layer in the Labrador Sea may have been the melting of Labrador Sea Ice with the increase of solar heating as the summer approaches (Wu et al., 2008). In the Labrador Sea there are two distinct periods within the seasonal cycle of water column stability: a stratification period and a convection period. Stratification (roughly May–December) is associated with a warming and an increase in salt content of the lower layer (200 - 1300 m) and a freshening of the surface layer (0 - 200 m). During convection (January–April), these trends are reversed (Straneo, 2006). During the period of this investigation, water properties were similar to the stratification period (CTD profiles, only upper 200 m are shown, Fig. 5) and thus further confirm that the Labrador Sea was in a early spring situation during the sampling period (Wu et al., 2008). In contrast, all other stations over the Irminger Basin, Reykjanes Ridge and Iceland Basin remained in a winter situation with a deep mixed layer approximately extending down to 500 m depth (CTD profiles, not shown). However , the southern-most part of the Irminger Basin had water properties similar to the adjacent Labrador Sea. Talley and McCartney (1982) noted that Labrador Sea water, that may occur in mid-depth in the Labrador Sea might potentially be advected into the Irminger Basin. I can therefore be reasonably sure that observed similarity of water properties between the Labrador Sea and southern-most part of Irminger Basin was due to the advective-transport of water. Labrador Sea surface water, which entered into the Irminger Basin, then underwent winter mixing and was distribute homogenously throughout the upper mixed-layer. Accordingly, the zooplankton distribution in the Labrador Sea corresponded to a early spring situation with high

abundances of mesozooplankton, whereas the Reykjanes Ridge and Iceland Basin mesozooplankton corresponded mostly to a winter situation with generally lower mesozooplankton abundances. However, even though the water column over the Irminger Basin remained in a winter situation, the observed relatively high mesozooplankton abundance further confirmed that mesozooplankton-enriched LSSW may have been advected into the Irminger Basin.

The reason for observed high abundance of the mesozooplankton over the Labrador Sea may be due to the influx of a new generation of early copepodites stages from the April-June reproduction period (Labrador Sea monitoring group, 2006) into the upper layer. Previous studies in the eastern Labrador Sea have shown that peak abundances of early copepodites stages were reached in late May (Labrador Sea monitoring group, 2006) with an average of 8940 m^{-3} individuals of *Calanus finmarchicus* in the upper 100 m. This study reported an average of 2884 ind m^{-3} of small-sized zooplankton within upper 100 m. Moreover, zooplankton net samples have confirmed that *C. finmarchicus* was the dominant zooplankton species in the study area (own observation). The relatively high zooplankton abundances indicate that the spring bloom in the LSSW had progressed.

4.2 Interpretation of biovolume spectra

The intercepts of the biovolume spectra in AtW over the Iceland Basin and Reykjanes Ridge were low, and comparable to the spectra obtained from a Atlantic water in Polar front in the Barents Sea in April/May, while the intercepts of the biovolume spectra in the Labrador Sea and AtW over northern-most Irminger Basin were high, but lower than those observed in a highly productive Polar front in Barents Sea in April/May (Basedow et al., 2010). The biovolume

spectra thus indicating a potentially low productivity in the Iceland Basin and Reykjanes Ridge and a potentially higher productivity in the Labrador Sea and Irminger Basin. Hence, the spectra further confirm that the zooplankton community in AtW still remained in a winter situation but not in northern-most Irminger Basin. On the other hand elevated productivity in the LSSW over Labrador Sea indicating a pre-bloom situation. The observed enhanced productivity in the Irminger Basin   probably can be a situation with temporary enrichment in zooplankton abundances due to advective - transport of zooplankton enriched Labrador Sea surface water into the Irminger Basin.

4.3 Baseline to quantify the TPs based on stable isotope analyses

The objective to define a baseline for the food web, is to reflect the isotopic signatures of the primary source of production (Cabana & Rasmussen 1994). Selection of an appropriate baseline to estimates trophic positio is one of the most complex task in the application of stable isotopes to trophic studies (Post, 2002). The complexity is more pronounced in plankton studies, as it is very difficult to isolate pure samples of primary producers (TL= 1) from plankton communities. Filterable seston may include a mixture of phytoplankton, primary consumers and non-living particles, each component having its own isotopic signature. Thus each represents a different trophic position within the food web (Muñoz, 2007). In the current study, I used the isotopic signature of the 55 - 200 μm size fraction as a baseline to estimate TPs of mesozooplankton size classes. However, microscopic examination revealed that this size fraction included a mixture of phytoplankton and primary consumers (bioseston). Therefore, a mean TP of 1.5 was assigned to the baseline size fraction by assuming a trophic position of 1 and 2 for phytoplankton and primary consumers respectively. However, using bioseston as a baseline is methodologically straightforward, but it is only applicable when mesozooplankton species feed non-selectively on

bioseston. Conversely, if mesozooplankton species feed selectively on particular seston group/groups, using bioseston as the baseline may cause erroneous calculations of mesozooplankton trophic position, because taxonomic groups in bioseton are isotopically distinct (e.g. phytoplankton, ciliates, flagellates) (Muñoz, 2007).

4.4 δ^{15}N trophic enrichment variability

There is currently more confidence in the use of δ^{15}N as a trophic level indicator compared to δ^{13}C, because these isotopic changes per trophic level are larger (Fry and Quinones, 1994). It has been repeatedly documented that a wide variety of animals from aquatic habitats are enriched in δ^{15}N by ~1.5‰- 4.5‰ relative to their diet, with an overall average enrichment of ~3.4%o for animals in general (Montoya et al. 1990, 1992; Kling et al. 1992). However, in this study, the observed maximum stepwise enrichment of δ^{15}N among size classes was 2.6‰. In addition the zooplankton community did not show any consistent stepwise enrichment of δ^{15}N from small to large sized zooplankton. Based on the assumption of 3.4‰ per trophic level, a 4-level system (e.g. in this a study food chain including the base line size fractionated group (55 - 200 μm sized class) $\longrightarrow$ small zoooplankton $\longrightarrow$ medium zooplankton $\longrightarrow$ large zooplankton) should result in an across food chain δ^{15}N increase of around (3.4‰ × 4) 13.6‰. While the observed isotopic spread (ranged between 0.7 and 6.7‰) is clearly below of 13.6‰, that was predicted by the assumption. There are some biological evidences to support observed lower stepwise δ^{15}N enrichment (< 3.4‰) and isotopic spread in the study area. Firstly, Dunton et al.(1989) found that food webs where the bacterial processing of detrital matters is important, δ^{15}N changes across trophic positions seem to be considerably smaller than 3.4 ‰, thus δ^{15}N may not be a reliable tracers of trophic position at lower trophic levels in detritus-based food webs. However,

there are practical difficulties in measuring $\delta^{15}N$ of phytoplankton and the microbial loop organisms separately, thus TPs cannot be determined independently. Furthermore, there is little existing information about isotopic changes in these smaller organisms, which play an important role in marine planktonic food webs (Fry and Quinones, 1994). Secondly, in studies on benthic and kelp-associated communities, Kaehler et al. (2000) observed that those communities exhibited no discrete trophic levels (assuming 3 - 4‰ per trophic level), suggesting a higher degree of omnivory. In the case of my study, both factors, i.e. a detritus-based food web and mesozooplankton omnivory could be the possible causes for the observed low stepwise trophic enrichment and isotopic spread across trophic levels. The hydrographical conditions prevailing in the study area (winter/early spring) during the period of investigation may favor for both biological processes including recycling matter through the microbial loop organisms and triggering omnivorous feeding behavior of mesozooplankton community due to the scarcity of their most preferred prey items (Kleppel, 1993; El-Sabaawi et al., 2010; Paulsen, 2013). In this study, 3.4 ‰ per trophic level was used to estimate TPs, a value typically used for the trophic studies (Vander Zanden and Rasmussen, 2001; Post, 2002) as unawareness of precise isotopic enrichment between trophic levels.

4.5 Spatial variability of mesozooplankton $\delta^{15}N$

The results confirmed the presence of geographical differences in zooplankton $\delta^{15}N$, but did not show any longitudinal gradient (Fig. 8). The geographic differences were more pronounced at lower trophic levels among small zooplankton, which may feed on phytoplankton or microbial loop organisms, and reflected that a different zooplankton food web may have operated simultaneously in the study area (Hannides et al., 2009). For instance, the zooplankton

community $\delta^{15}N$ was the highest at the Reykjanes Ridge and the lowest in the Iceland Basin (station 127), but these differences were not large. This may reflect differences in the trophic structure and energy conversion efficiency or indicate the availability of a $\delta^{15}N$ enriched nitrogen source at the Reykjanes Ridge, which may have been utilized by higher consumers of the region (Dunton et al., 1989).

4.6 Comparison of trophic positions: biovolum spectrum vs stable isotope

The approach to estimate TPs, based on stable isotope analyses showed community TPs of the study area ranging from 1.5 to 3.5, and thus within the range of primary and secondary consumers. However, TPs did not link with the water mass characteristics of the study area. In contrast, community TPs computed based on biovolume spectrum analyses ranged from 3.3 to 5.9 and almost link to the water mass characteristics. The range of community TP was much higher than those generated by stable isotope analysis. Moreover, TPs of small and large sized mesozooplankton groups also had relatively high values for biovolume spectrum analysis (Table 5). Several factors may explain the discrepancies between the two methods. These include : 1) a time lag between the two sampling methods, 2) differences in assimilation efficiencies of the mesozooplankton, 3) a responsiveness of the biovolume spectrum to the recycling processes driven by microbial community, that was not detected precisely by the stable isotope analyses.

4.6.1 Time lag between the two sampling methods

During the cruise, net samples were not collected in synchrony with the LOPC deployment, which produced a time lag between the two sampling methods (Table 1). Time inconsistency may possibly cause zooplankton density disparities between sampling data obtained from two

methods. Time inconsistencies between samples are likely to be a major problem in advective environments with spatially heterogeneous populations, particularly zooplankton, since they are incapable of maintaining their position along with water movements (Speirs et al., 2004). In the current study, hydrographical data supported for advective transport of LSSW into the southern-most Irminger Basin, but provided no evidences of advection in other study regions. Unfortunately, there is no knowledge of spatial homogeneity/heterogeneity of zooplankton communities during the period of study. However, at all stations mesozooplankton abundances recorded by the LOPC were well proportionate with the plankton net samples (own observation). Moreover, the observed pattern of mesozooplankton TPs indicate that there should be a dependable factor to yield higher TPs for biovolume spectrum analyses, instead of random variations due to consequences of advection and zooplankton patchiness.

4.6.2 Differences in assimilation efficiencies of the mesozooplankton

In order to estimate TPs based on biovolume spectrum theory, a constant assimilation efficiency of 70% was used for all size classes. This may cause overestimation or underestimation of TPs because zooplankton assimilation efficiency depends on a number of factors including nutrient content in food, availability of organic compounds, food source, species, body weight, temperature and development stage (Mauchline,1998; Mayzaud et al.,1998; Almeda et al.,2011). For instance, *Calanus pasificus* assimilation efficiency can range from 68.5 to 85.4% for carbon and 73.9 to 92.5% for nitrogen (Landry et al., 1984). The assimilation efficiency of herbivorous zooplankton is assumed to range from 60 to 70% (Pasternaki et al., 2002). For carnivores zooplankton, assimilation efficiency may be as high as 98% (Mauchline, 1998). However TPs estimations based on biovolume spectrum theory do not strongly depend on assimilation

efficiency, e.g. assuming assimilation efficiency varying by ±20% would change trophic position only by 0.2.Thus, assimilation efficiency is not a reliable factor in explaining the observed trophic variations between biovolume spectrum and stable isotope analysis.

4.6.3 Responsiveness of the biovolume spectrum to the recycling processes driven by microbial community

The most reasonable and straightforward factor for the observed discrepancies of TPs estimations is that the biovolum spectrum can trace microbial loop linkages, which cannot be distinguished by stable isotope analyses due to methodological difficulties. According to equation 4 (section 2.8.1), the number of TPs estimated from the biovolume spectrum mainly depends on the slope of the spectrum, assuming that the assimilation efficiency is constant for the all size classes. On the other hand, the slope of the spectrum is determined by the energy fluxes through the system (Platt and Denman, 1978; Zhou, 2006). Energy to the system can be supplied in two ways, 1) direct transfer from primary producers such as phytoplankton (new energy), and 2) internal recycling of dissolved organic matters (DOMs) by the microbial loop organisms (regenerated energy). A substantial amount of new energy by the primary producers may be lost from the system due to population metabolism while the energy propagates along the spectrum, resulting in a steeper slope of the spectrum. In a system with a feedback mechanism through the microbial loop, the system energy loss is low and may result in a flatter slope of the biovolume spectrum. Therefore, biovolume spectra with flatter slopes reflect a relatively high trophic number of the mesozooplankton community due to microbial loop linkages (Fig. 11) (Zhou, 2006).
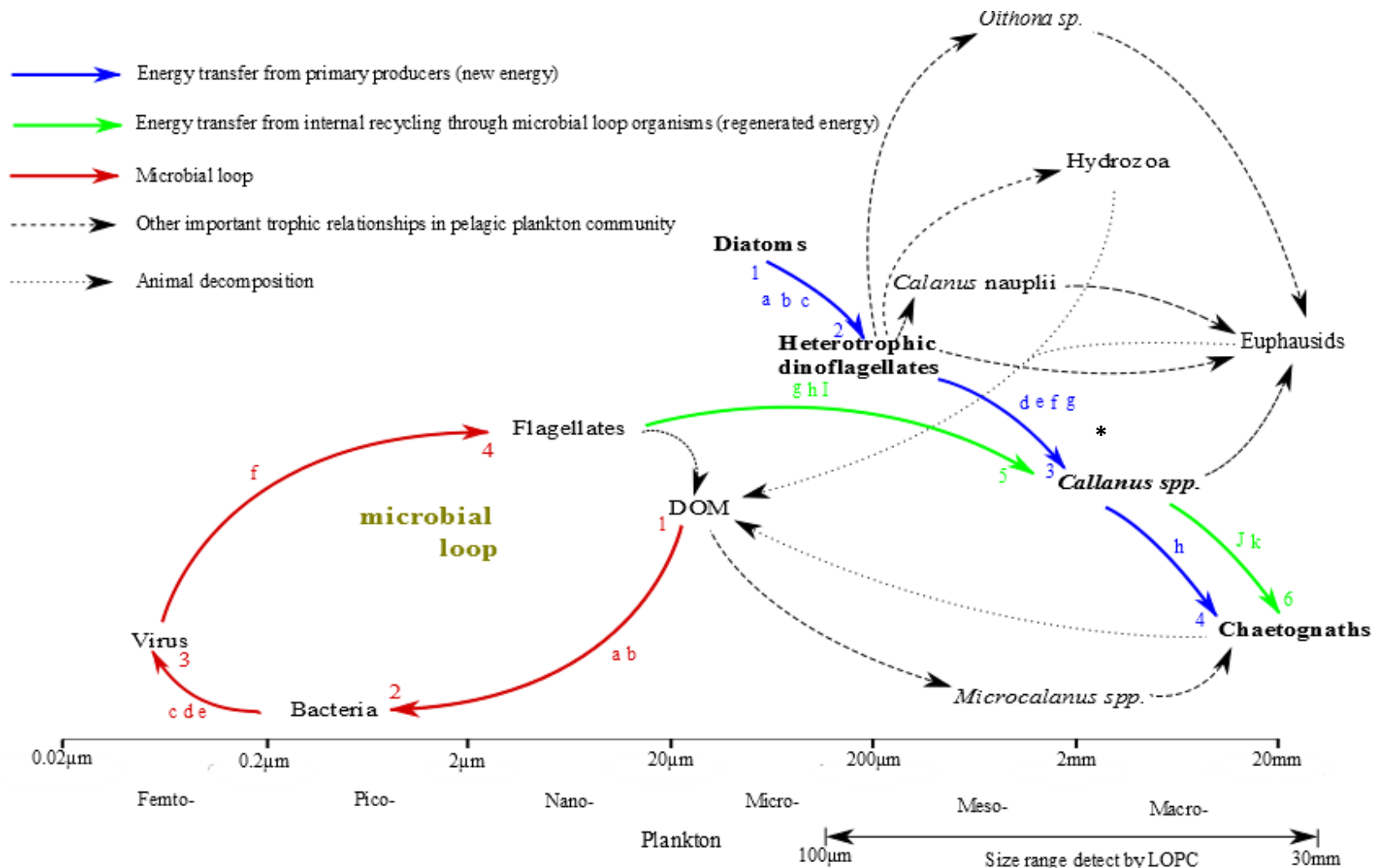
Figure 11 : Hypothetical representation of marine pelagic planktonic food web, explaining the reason for relatively higher TP computation by the biovolume spectrum analysis compared to stable isotope analysis

* *Callanus* spp. received energy from both primary producers and microbial loop organisms. But stable isotope analysis could not trace these two energy source separately, therefore, by assuming classical trophic relationship of Diatom ⟶ Ciliates ⟶ *Callanus* spp. ⟶ Chaetognaths, *Callanus* spp. received TP of 3 based on stable isotope analysis. However biovolume spectrum method can trace both energy sources seperately and compute TP of 4 (average of 5 + 3). Therefore, biovolume spectrum can have higher TP with the increase of microbial loop linkages.

(a: Cherrier et al., 1996; b: Baines and Pace, 1991; c, f: Fuhrman, 1999; d: Steward et al., 1996; e: Middelboe et al., 2003; g: Turner et al., 2001; h: Castellani et al.,2005a; h, J: Duró and Saiz, 2000; k: Feigenbaum & Maris 1984 a: Strom and Morello, 1998; b: Saito et al., 2006; c: Jeong et al., 2010; d: Mayor et al.,2006; e: Irigoien et al.,1998; f: Harris et al.,2000; g, I: Castellani et al.,2008)

39

4.6.3a Modeling approach to trace microbes driven recycling processes

In this study, I have observed that the mean trophic position increment (MTPI, section 2.9) of the mesozooplankton size classes increased as small < large < All (Table 7). Further, MTPI was more pronounced in LSSW than in AtW (Table 8). Therefore, based on differences in MTPI and the slopes of the biovolume spectra in relation to the different water masses in the study area, a hypothetical model was developed to explain those observed variations.

Table 8: MTPI for small (S), large (L) and whole (All) zooplankton community in LSSW and AtW. MTPI is more pronounced in LSSW due to many microbial linkages.

Size class	LSSW			AtW		
	Mean TP		MTPI	Mean TP		MTPI
	BST	SIA	BST/SIA	BST	SIA	BST/SIA
S	2.5	2.1	1.2	2.5	2.0	1.3[a]
M	-	-	-	-	-	-
L	5.8	2.5	2.3	2.8	2.6	1.1[b]
All	5.0	2.1	2.4	3.7	2.3	1.6

a & b - according to the hypothytical model (scenario 1) microbial loop can be link to the small size class. Thus, these small zooplankton may fed by both new and regenerated energy and yield relatively a flatten slope. Therefore, MTPI is higher for that portion of the spectrum, but when this energy propogate along the spectrum and reach the large zooplankton, a considerable amount of energy may be lost , resulting in a relatively steeper slope and low MTPI for large- sized zooplankton. In this particular situation MTPI changed as S >L < All.

Model interpretation

The model is based on the assumption that, MTPI occurred entirely due to the internal recycling of the matter by microbial loop organisms. As a result, the Mean Trophic Position Increment (MTPI) can be proportionate to the number of microbial loops within the system and slope of the given spectrum (according to equation 4). Based on different slopes observed for the biovolume spectra, 3 possible scenarios were proposed,

Scenario 1

Equivalent sperical diameter (mm)

slope: -0.62
n: 3.9

System Energy loss - High
(from whole zooplankton community)

Source 1
Phytoplankton → Small zooplankton → Medium zooplankton → Large zooplankton
Source 2
Nano flagellates
DOM
Microbial loop
Bacteria
Metabolism

# of microbial loop - 01

Scenario 2

Equivalent sperical diameter (mm)

slope: -0.41
n: 5.9

System Energy loss - Low
(from whole zooplankton community)

Source 1
Phytoplankton → Small zooplankton → Medium zooplankton → Large zooplankton
Source 2
DOM
Microbial loop
Bacteria
Nano flagellates
Metabolism
DOM
Microbial loop
Bacteria
Nano flagellates
Source 2

# of microbial loop - 02

Scenario 3

Equivalent sperical diameter (mm)

slope: -0.71
n: 3.4

S ← → M ← → L

System Energy loss - High
(highest from S and M zooplankton community)

Source 1
Phytoplankton → Small zooplankton → Medium zooplankton → Large zooplankton
Metabolism
DOM
Microbial loop
Bacteria
Nano flagellates
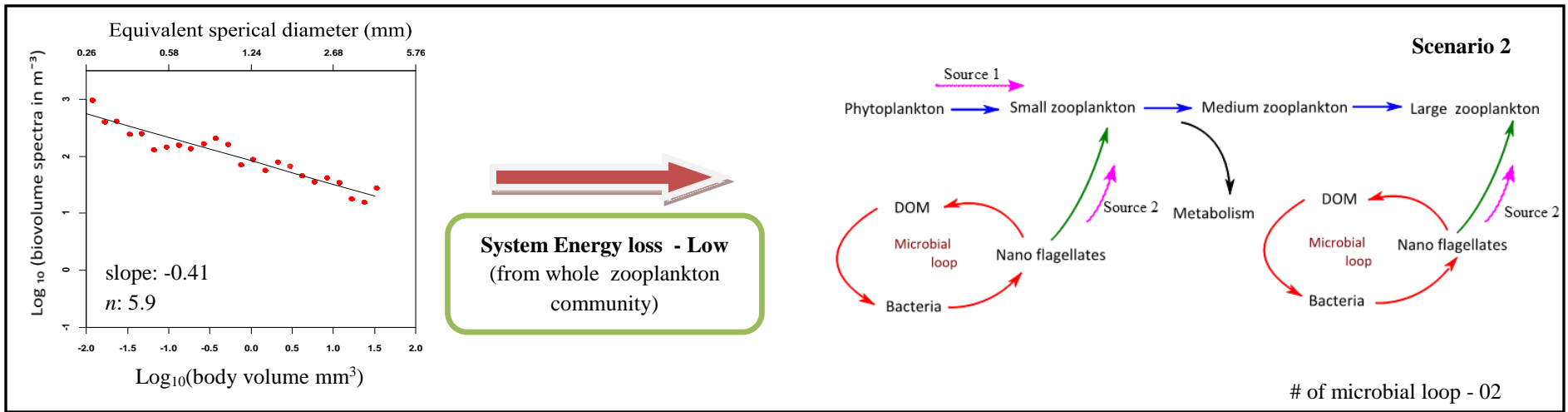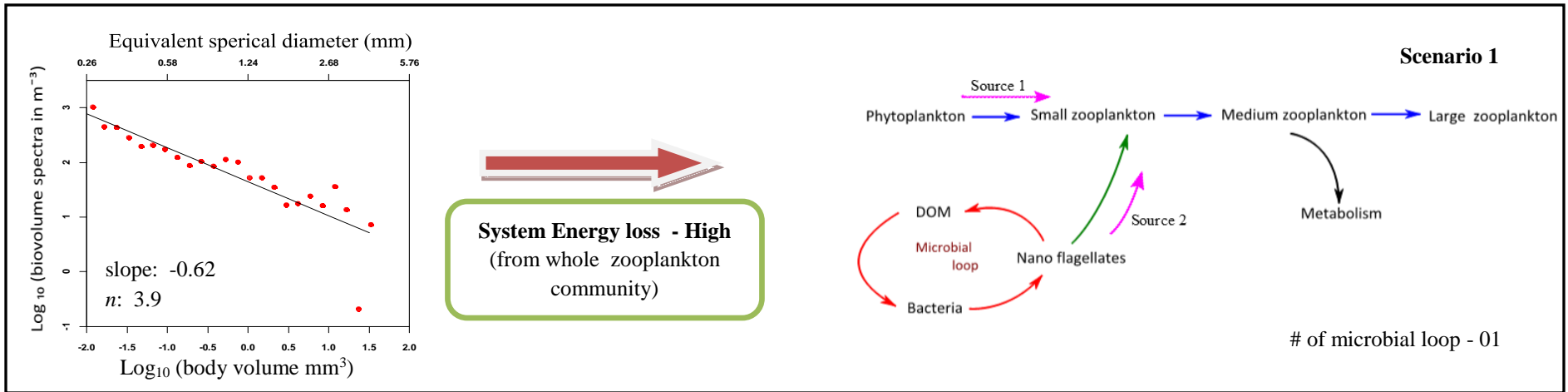Source 2

# of microbial loop - 01

Figure 12: Hypothetical model used to illustrate, 1) observed TP deviations between the biovolume spectrum analysis and stable isotope analysis, 2) relationship between shape of the spectrum Vs microbial loop linkages. Minimum number of microbial loops have been used to simplify data interpretation and presentation.

Energy source
Source 1 - New energy
Source 2 - Regenerated energy
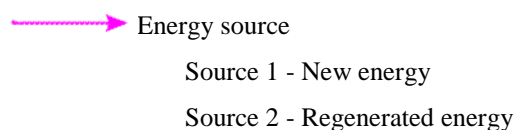
Scenario 1: This can be applied to a spectrum with a relatively steep biovolume spectrum slope. In this, microbial processes are at minimum. However, few microbial loops can be linked to the base of the spectrum (small size class), but not at medium or large size classes. Therefore, energy lost from the system is high. This scenario could be applied to the observed biovolume spectra with steeper slopes in AtW of the study area (stations 126,127,132 and 133).

Scenario 2: The biovolume spectrum slope is relatively flat and microbial processes are at maximum. Microbial loops can be linked to any part of the spectrum. Due to feedback mechanisms by microbial loops, energy loss from the system is at minimum and biomass recycling internally several time. This scenario fits to the observed spectra with flat slopes in LSSW in the northwest Labrador Sea (station 135) and southern-most part of the Irminger Basin (station 134)

Scenario 3: Biovolume spectrum slope is steeper as scenario 1, but few microbial loops can occur and alter certain parts of the biovolume spectrum, thus a relatively flat slope results for that particular part due to the additional energy supply from the regenerated energy. This can be the prevailing situation in station 137 in the Labrador Sea, which has a steeper slope for the entire biovolume spectrum, and a flatter slope for the spectrum of large size class. Here, small and medium sized zooplankton utilized energy only from primary producers (fed herbivorously), therefore the slope was steepest for that part of the spectrum. Large

zooplankton depended on both new and regenerated energy, thus the biovolume spectrum slope was flat in that size range.

This hypothetical model well explained the observed variations in the biovolume spectra and TPs in relation to different water masses in the study area. According to the model, the LSSW had high microbial activities, where the AtW had relatively low microbial activities. Paulsen (2013) also noted that microbial components are more dominant in the pelagic system, during pre-bloom conditions and lower during winter in the subpolar North Atlantic Ocean. Therefore, predictions by the model on microbial activities in relation to the two water masses, fit well with previous findings. However, the model is based on limited data and few environmental scenarios. Hence, in the future, it would be desirable to test the validity of the model by more comprehensive study including different environmental conditions.

4.7 Trophic mismatch and related consequences

The results of this study showed that the LSSW maintained a relatively a high zooplankton biomass, even though phytoplankton biomass remained very low during the study period. This can be likely due to timing and trophic mismatch of marine plankton, e.g. asynchrony between the spring phytoplankton bloom and emergent of new generation of early copepodites stages in to the surface mixed layer. Edwards and Richardson (2004) also noted a mismatch between trophic levels and functional groups due to the consequences of ongoing climate changes. Fuel to maintain high zooplankton biomass in the LSSW, there should be another reliable energy source despite energy from primary producers, thus suggesting a microbial loop dominated zooplankton food webs in LSSW during the pre-bloom condition as predicted by the model. Paulsen (2013) also emphasis the importance of nano-sized microorganisms as a consistent food source of

copepods during the pre-bloom period in Subpolar North Atlantic Ocean. However, high grazing pressure by the mesozooplankton can be a another possible reason for the observed low phytoplankton biomass in the LSSW, but observed relatively flatter slopes of the bivolume spectra in the region confirmed availability of recycling processes, driven by microbial community.

4.8 Trophic structure of the study area: what determined by the two methods

Overall, this study elucidate that the biovolume spectrum can yield higher TP due to presence of microbial loop linkages. The results of hypothetical model illustrates microbial loops based planktonic food webs were more pronounced in LSSW during the pre-bloom condition. Stable isotope analyses showed a lack of stepwise $\delta^{15}N$ enrichment among zooplankton size classes as observed in previous studies (Montoya et al. ,1992; Fry and Quinones, 1994), thus indicated only a modest change in trophic position across the size classes of the mesozooplankton community. This small TP change is consistent with the idea of zooplankton omnivory in unstructured food web (Isaacs, 1972; Fry and Quinones, 1994). However, stable isotope analyses were not suited to detect microbial based trophic dynamics in the mesozooplankton community, because of practical difficulties to measuring isotopic signature of microbes and primary producers separately (Fry and Quinones, 1994). In contrast, biovolume spectrum analyses is more perceptive to source of energy flux through the system. As a result, biovolume spectrum method can potentially trace the trophic dynamics in mesozooplankton community fueled by both new (priamary producers) and regenerated energy (microbial loop)

5. CONCLUSIONS

This study demonstrated for the first time, that the combined usage of biovolume spectrum and stable isotope analyses provided a powerful approach to assess the relationship between trophic dynamics of the mesozooplankton community and the microbial loop in relation to different environmental conditions. It also illustrate that biovolume spectrum theory was a reliable method to describe trophic relationships of planktonic ecosystems. Moreover, the hypothetical model developed in this study provided a baseline to evaluate a potential influence of microbial processes in order to determine the trophic structure of the mesozooplankton community. However, the results highlights the need for a more comprehensive study including trophic relationship covering many environmental scenarios to have a more complete view of trophic coupling between mesozooplankton and microbial loop organisms.

REFERENCES

Almeda, R., Alcaraz, M., Calbet, A., and Saiz, E., 2011. Metabolic rates and carbon budget of early developmental stages of the marine cyclopoid copepod *Oithona davisae. Limnol. Oceanogr.* 56 (1), pp. 403–414.

Baines, S.B.,and Pace, M.L., 1991. The Production of Dissolved Organic Matter by Phytoplankton and its Importance to Bacteria: patterns Across Marine and Freshwater Systems. *Limnology and Oceanography*, 36 (6),   pp. 1078-1090.

Barnard, R., Batten, S.D., Beaugrand, G. et al., 2004. Continuous Plankton Records: Plankton Atlas of the North Atlantic Ocean (1958–1999). II. Biogeographical charts. *Mar Ecol Prog Ser.,*sapply,2004, pp. 11-75.

Basedow, S.L., Edvardsen, A., and Tande, K.S., 2006. Spatial patterns of surface blooms and recruitment dynamics of *Calanus finmarchicus* in the NE Norwegian Sea. *Journal of Plankton Research*, 28(12), pp. 1181-1190.

Basedow, S.L., Tande, K.S., Norrbin, M.F., and Kristiansen, S.A., 2013. Capturing quantitative zooplankton information in the sea: Performance test of laser optical plankton counter and video plankton recorder in a *Calanus finmarchicus* dominated summer situation. *Progress in Oceanography, 108*, pp. 72-80.

Basedow, S.L.,Tande, K.S., and Zhou, M., 2010. Biovolume spectrum theories applied: spatial patterns of trophic levels within a mesozooplankton community at the polar front. *Journal of plankton research,* 32(8), pp. 1105-1119.

Beaugrand, G., Reid, P.C., Ibanez, F., Lindley, J.A. and Edwards, M., 2002. Reorganization of North

Atlantic Marine Copepod Biodiversity and Climate. *SCIENCE,* 296, pp. 1692-1694.

Cabana, G., and Rasmussen, J.B., 1994. Modeling food chain structure and contaminant bioaccumulation using stable nitrogen isotopes. *Nature (Lond.),* 372, pp. 255-257.

Carpenter, S.R., Kitchell, J.F., and Hodgson, J.R., 1985. Cascading trophic interactions and lake productivity. *BioScience*, 35, pp. 381-389.

Castellani,C., Irigoien,X., Harris R.P., et al., 2005a. Feeding and egg production of *Oithona similis* in the North Atlantic. *Mar. Ecol. Prog. Ser.*, 288, pp.173-182.

Castellani, C., Irigoien, X., Mayor, D.J., Harris, R.P., and Wilson, D., 2008. Feeding of *Calanus finmarchicus* and *Oithona similis* on the microplankton assemblage in the Irminger Sea, North Atlantic. *Journal of Plankton Research,*30 (10), pp. 1095-1116.

Cherrier, J., Bauer, J.E., and Druffe, E.R.M., 1996. Utilization and turnover of labile dissolved organic matter by bacterial heterotrophs in eastern North Pacific surface waters. *Mar Ecol Prog Ser,* 139, pp. 267-279.

Cleary, A.C., Durbin, E.G., and Rynearson, T.A., 2012. Krill feeding on sediment in the Gulf of Maine (North Atlantic). *Mar Ecol Prog Ser.*455, pp. 157-172.

Cohen, R.E., and Lough, R.G., 1981. Length-Weight Relationships for Several Copepods Dominant in the Georges Bank-Gulf of Maine Area. *J. Northw. Atl. Fish. Sci*., 2 , pp. 47-52.

Conway, D.V.P., 2012. Identification of the copepodite developmental stages of twenty-six North Atlantic copepods. Occasional Publications. Marine Biological Association of the United Kingdom, No. 21 (revised edition), Plymouth, United Kingdom, pp. 35.

Dunton, K.H., Saupe, S.M., Golikov, A.N., Schell, D.M., and Schonberg, S.V., 1989. Trophic relationships and isotopic gradients among arctic and subarctic marine fauna. *Mar Ecol Prog Ser,* 56, pp. 89-97.

Duro, A., and Saiz, E., 2000. Distribution and trophic ecology of chaetognaths in the western Mediterranean in relation to an inshore–offshore gradient. *Journal of Plankton Research,* 22 (2), pp. 339-361.

Edvardsen, A., Zhou, M., Tande, K. et al., 2002. Zooplankton population dynamics: measuring in situ growth and mortality rates using an Optical Plankton Counter. *Mar. Ecol. Prog. Ser.*, 227, pp. 205–219.

Edwards, M., and Richardson, A. J., 2004. Impact of climate change on marine pelagic phenology and trophic mismatch. *Nature,* 430, pp. 881-883.

El-Sabaawi, R.W., Sastri, A.R., Dower, J.F., & Mazumder, A., 2010. Deciphering the Seasonal Cycle of Copepod Trophic Dynamics in the Strait of Georgia, Canada, Using Stable Isotopes and Fatty Acids. *Estuaries and Coasts*,33 (2010), pp.738–752.

Falkowski, P.G., Scholes, R.J., Boyle, E., Canadell, J. and 13 others, 2000 .The global carbon cycle: a test of our knowledge of earth as a system. *Science* , 290, pp. 291–296.

Feigenbaum, D. L., and Maris, R. C., 1984. Feeding in the Chaetognatha..*Oceanogr. Mar. Biol. Annu. Rev*., 22, pp. 343–392.

Forest, A., Stemmann, L., Picheral, M., Burdorf, L., Robert, D., Fortier, L., and Babin, M., 2012. Size distribution of particles and zooplankton across the shelf-basin system in southeast Beaufort Sea: combined results from an Underwater Vision Profiler and vertical net tows. *Biogeosciences*, 9, pp. 1301-1320.

France, R.L.,and Peters, R.H., 1997. Ecosystem differences in the trophic enrichment of ^{13}C in aquatic food webs. *Can. J. Fish. Aquat. Sci*., 54, pp. 1255-1258.

Fry, B., and Quinones, R. B., 1994. Biomass spectra and stable isotope indicators of trophic level in zooplankton of the northwest Atlantic. *Marine Ecology Progress Series*, 112, pp. 201-204.

Fuhrman, J.A., 1999. Marine viruses and their biogeochemical and ecological effects. NATURE, 399, pp. 541-548.

Gallienne, C.P., and Robins, D.B., 2001. Is *Oithona* the most important copepod in the world's oceans?. *Journal of Plankton Research,* 23(12), pp. 1421-1432.

Gibbons, M.J., and Richardson, A.J., 2009. Patterns of jellyfish abundance in the North Atlantic. *Developments in Hydrobiology,* 206, pp. 51-65.

Gislason, A., 2003. Life-cycle strategies and seasonal migrations of oceanic copepods in the Irminger Sea. *Hydrobiologia ,*503, pp.195–209.

Greene, C.H., 1988. Foraging tactics and prey-selection patterns of omnivorous and carnivorous calanoid copepods. *Hydrobiologia ,*167, pp. 295 - 302.

Hannides, C.C.S., B.N. Popp, M.R. Landry, and B.S. Graham. 2009. Quantification of zooplankton trophic position in the North Pacific Subtropical gyre using nitrogen stable isotopes. *Limnology and Oceanography,* 54(1), pp. 50–61.

Harris, R.P., Irigoien,X., Head, R.N., and 6 others, 2000. Feeding, growth, and reproduction in the genus *Calanus. ICES Journal of Marine Science,* 57, pp. 1708–1726.

Head, E.J.H., Harris, L.R., and Yashayaev, I., 2003. Distributions of *Calanus* spp. and other mesozooplankton in the Labrador Sea in relation to hydrography in spring and summer (1995–2000). *Progress in Oceanography* ,59 (2003) , pp. 1–30.

Heath, M.R., 1995. Size spectrum dynamics and the planktonic ecosystem of Loch Linnhe. *ICES J Mar Sci* ,52, pp. 627–642.

Henson, S.A., Robinson, I., Allen, J.T., and Waniek, J.J., 2006. Effect of meteorological conditions on interannual variability in timing and magnitude of the spring bloom in the Irminger Basin, North Atlantic. *Deep-Sea Research I*, 53 (2006), pp. 1601–1615.

Herman, A. W., 1988. Simultaneous measurement of zooplankton and light attenuance with a new optical plankton counter. *Cont. Shelf Res.*, 8, pp. 205–221.

Herman, A. W.,1992. Design and calibration of a new optical plankton counter capable of sizing small zooplankton. *Deep Sea Res.*, 39, pp. 395-415.

Herman, A.W., Beanlands, B., and Phillips, E.F., 2004. The next generation of Optical Plankton Counter: the Laser-OPC. *J. of Plankton research*, 26(10), pp. 1135-1145.

Herman, A.W., Cochrane, N.A., and Sameoto, D.D., 1993. Detection and abundance estimation of euphausiids using an optical plankton counter. *Marine Ecology Progress Series*,94, pp. 165–173.

Ho, C., and Marra, J., 1994. Early-spring export of phytoplankton production in the northeast Atlantic Ocean. *Marine Ecology Progress Series,* 114, pp. 197-202.

Irigoienl, X., Head, R., Klenke, U., and 5 others, 1998. A high frequency time series at weathership M, Norwegian Sea, during the 1997 spring bloom: feeding of adult female *Calanus finmarchicus. Mar Ecol Prog Ser,*172, pp. 127-137.

Irigoien, X., Titelman, J., Harris, R.P.,Harbour, D., and Castellan, C., 2003. Feeding of *Calanus*

*finmarchicu*s nauplii in the Irminger Sea. *Mar Ecol Prog Ser,*262, pp. 193-200.

Isaacs, J. D., 1973. Potential trophic biomasses and trace-substance concentration in unstructured marine food webs. *Marine Biology*, 22, pp. 97-104.

Iversen, K.R., and Seuthe, L., 2011. Seasonal microbial processes in a high-latitude fjord (Kongsfjorden, Svalbard): I. Heterotrophic bacteria, picoplankton and nanoflagellates. Polar Biology , 34(5), pp. 731-749.

Jardine, T.O., Kidd, K.A. and Fisk, A.T., 2006. Applications, considerations, and sources of uncertainty when using stable isotope analysis in ecotoxicology. *Environmental Science and Technology* ,40, pp. 7501-7511.

Jeong, H.J., Yoo, Y.D., Kim, J.S., and 3 others, 2010. Growth, Feeding and Ecological Roles of the Mixotrophic and Heterotrophic Dinoflagellates in Marine Planktonic Food Webs. *Ocean Sci. J*., 45(2), pp. 65-91.

Johns, D.G., Edwards, M., and Batten, S.D., 2001. Arctic boreal plankton species in the Northwest Atlantic. *Can. J. Fish. Aquat. Sci*., **58**, pp. 2121–2124.

Kaehler, S., Pakhomov, E.A., and McQuaid, C.D., 2000. Trophic structure of the marine food web at the Prince Edward Islands (Southern Ocean) determined by δ^{13}C and δ^{15}N analysis. *Mar Ecol Prog Ser,*208, pp. 13-20.

Kleppel, G.S., 1993. On the diets of calanoid copepods. *Marine Ecology Progress Series* 99(1-2), pp.183–195.

Kling, G.W., Fry, B., and O.Brien, W.J., 1992. Stable isotopes and planktonic trophic structure in arctic lakes. *Ecology*, 73, pp. 561-566.

Krause, M., Fock, H., Greve, W., and Winkler, G., 2003. North Sea Zooplankton: a Review. *Senckenbergiana maritima,*33, pp. 71-204.

Labrador Sea monitoring group, 2006. *Status of the Labrador Sea. annual report* 2006, Bedford Institute of Oceanography.

Lajtha, K., and Michener, R.H., 1994. Stable isotopes in ecology and environmental science, Vol. Blackwell scientific publications, Oxford.

Landry, M.R., Hassett, R.P., Fagerness, V., Downs, J., and Lorenzen, C.J., 1984. Effect of food acclimation on assimilation efficiency of *Calanus pacificus*. *Limnology and Oceanography*, 29, pp. 361-364.

Layman, C.A., Araujo, M.S., Boucek, R., and 9 others, 2011. Applying stable isotopes to examine food-web structure: an overview of analytical tools. *Biol. Rev.* (2011).

Lazier, J.R.N., Hendry, R.M., Clarke, R.A., Yashayaev, I., and Rhines, P., 2002. Convection and restratifica tion in the Labrador Sea, 1990–2000. *Deep-Sea Research Part I ,49(10),* pp.1819–1835.

Letessier, T.B., Falkenhaug, T., Debes, H., Bergstad, O.A., and Brierley, A.S., 2011. Abundance patterns and species assemblages of euphausiids associated with the Mid-Atlantic Ridge, North Atlantic. *Journal of Plankton Research,* 33(10), pp. 1510-1525.

Lindeman, R.L., 1942. The tropho-dynamic aspect of ecology. *Ecology*, 23, pp. 399-418.

Malmberg, S., 2004. *The Iceland Basin: Topography and Oceanographic Features*. Marine Research Institute. Report 109.

Marra, J., 1995. Primary production in the North Atlantic: measurements, scaling, and optical determinants. *Phil. Trans. R. Soc. Lond. B.,* 348, pp. 153 - 160.

Mauchline, J., 1998. The biology of calanoid copepods. *Advances in Marine Biology* 33, pp. 701–710.

Mayor, D.J., Anderson, T.R., Irigoien, X., and Harris, R., 2006. Feeding and reproduction of *Calanus finmarchicus* during non-bloom conditions in the Irminger Sea. *Journal of Plankton Research,* 28 (12), pp. 1167-1179.

Mayzaud, P., Tirelli, V., Bernard, J.M., Roche-Mayzaud, O., 1998. The influence of food quality on the nutritional acclimation of the copepod *Acartia clausi. J. Mar. Sys.,* 15, pp. 483-494.

Meyer-Harms, B., Irigoien, X., Head, R., and Harris, R., 1999. Selective feeding on natural phytoplankton by *Calanus finmarchicus* before, during,and after the 1997 spring bloom in the Norwegian Sea. *Limnol. Oceanogr.,* 44(1), pp.154–165.

Middelboe, M., Riemann, L., Steward, G.F., Hansen, V., and Nybro, O., 2003. Virus-induced transfer of organic carbon between marine bacteria in a model community. *Aquat Microb Ecol.,* 33, pp. 1–10.

Montoya, J. P., Horrigan, S. G., and McCarthy, J. J., 1990. Natural abundance of 15N in particulate nitrogen and zooplankton in the Chesapeake Bay. *Marine Ecology Progress Series*, 65,pp. 35-61.

Montoya, J. P., Wiebe, P.H., and McCarthy, J. J., 1992. Natural abundance of ^{15}N in particulate nitrogen and zooplankton in the Gulf Stream region and Warm-Core Ring 86A. *Deep-Sea Res. (suppl. 1)*, 39, pp 363-392.

Muñoz, C.A., 2007. Assessing mesozooplankton trophic levels in the Baltic Sea and North Sea: A stable isotope study. Ph.D. Faculty of Mathematics and Natural Sciences :Christian-Albrechts-University Kiel.

Ogilvie, H. S., 1953. *COPEPOD NAUPLII* (U) - ICES
Available at: https://www. *info.ices.dk/products/fiche/Plankton/SHEET050.PDF*

Oresland, V., 1987. Feeding of the chaetognaths *Sagitta elegans* and *S. setosa* at different seasons in Gullmarsfjorden, Sweden. *Mar Ecol Prog Ser,*39, pp. 69-79.

Pasternaki, A., Riseri, C.W., Arashkevicha, E., Rat'kovaa, T., and Wassmamri, P., 2002. *Calanus* spp. grazing affects egg production and vertical carbon flux (the marginal ice zone and open Barents Sea). *Journal of Marine Systems,* 38 (2002), pp. 147-164.

Paulsen, L.M., 2013. *Pre-bloom dynamics of the Subpolar North Atlantic microbial food web*. MS.c. Joint Nordic Master's Programme in Marine Ecosystems and Climate. EURO-BASIN.

Peterson, B.J.,and Fry, B., 1987. Stable isotopes in ecosystem studies. *Annu. Rev. Ecol. Syst*. ,18, pp. 293 - 320.

Piontkovski, S., and Melnik, T., 2008. Mesozooplankton average length during Professor Vodyanitskiy cruise PV14. [online].
Available at: http://doi.pangaea.de/10.1594/PANGAEA.691592
(Accessed on 12 February 2014)

Planque, B., and Taylor, A.H., 1998. Long-term changes in zooplankton and the climate of the North Atlantic. *ICES Journal of Marine Science,* 55, pp. 644-654.

Platt, T. 1985. Structure of the marine ecosystem: Its allometric basis. In: R.E. Ulanowicz, and T. Platt ed*. Ecosystem theory for biological oceanography*. Can. Bull. Fish. Aquat. Sci., 213, pp. 55-64.

Platt, T., and Denman, K., 1977. Organisation in the pelagic ecosystem. *Helgolander Wiss Meeresunters,* 30, pp. 575-581.

Platt, T., and Denman, K.,1978.The structure of pelagic marine ecosystems. *Rapp. P.-V. Rèun. Cons. Int. Explor. Mer.*, 173, pp. 60–65.

Post, D. M., 2002. Using stable isotopes to estimate trophic position: models, methods, and assumptions. Ecology, 83, pp. 703-718.

Prince Edward Islands (Southern Ocean) determined by $\delta^{13}C$ and $\delta^{15}N$ analysis. *Mar Ecol Prog Ser,*208, pp. 13-20.

Prokopchuk, I., 2003. Mesozooplankton distribution, feeding and reproduction of *Calanus finmarchicus* in the western Norwegian Sea in relation to hydrography and chlorophyll *a* in spring. Knipovich Polar Research Institute of Marine Fisheries and Oceanography, (PINRO), The United Nations University.

Quinones, R. A., Platt, T., and Rodriguez, J., 2003. Patterns of biomass-size spectra from oligotropic waters of the Northwest Atlantic. *Prog. Oceanogr*, 57, pp. 405–427.

Quinones, R.A., 1994. A comment on the use of allometry in the study of pelagic ecosystem processes. *SCI.MAR.*, 58(1-2), pp. 11-16.

Rasmussen, J.B., Rowan, D.J., Lean, D.R.S., and Carey, J.H., 1990. Food chain structure in Ontario lakes determines PCB levels in lake trout (*Salvelinus namaycush*) and other pelagic fish. *Can. J. Fish. Aquat. Sci.*, 47,pp. 2030-2038.

Rodríguez, J. 1994. Some comments on the size based structural analysis of the pelagic ecosystem. *Sci. Mar.*, 58, pp. 1-10.

Rolff, C., 2000. Seasonal variation in $\delta^{13}C$ and $\delta^{15}N$ of size fractionated plankton at a coastal station in the northern Baltic Proper. *Marine Ecology Progress Series*, 203, pp. 47-65.

Rolff, C., and Elmgren, R., 2000. Use of riverine organic matter in plankton food webs of the Baltic Sea. *Mar. Ecol. Prog. Ser.*, 197, pp. 81-101.

Rounick, J.S., and Winterbourn, M.J., 1986. Stable Carbon Isotopes and Carbon Flow in Ecosystems. *BioScience*, 36 (3), pp. 171-177.

Saito, H, Ota, T, Suzuki, K., Nishioka, J., and Tsuda, A., 2006. Role of heterotrophic dinoflagellate Gyrodinium sp. in the fate of an iron induced diatom bloom. *Geophysical Research Letters*, 33.

Saiz, E., and Kioerboe, T., 1995. Predatory and suspension feeding of the copepod *Acartia tonsa* in turbulent environments. *Mar Ecol Prog Ser* ,122, pp. 147 - 158.

Sathyendranath, S., Longhurst, A., Caverhill, C.M., and Platt, T., 1995. Regionally and seasonally differentiated primary production in the North Atlantic. *Deep-Sea Research I*, 42 (10), pp. 1773-1802.

Sheldon, R.W., Prakash, A., and Sutcliffe, W.H.J., 1972. The size distribution of particles in the ocean. *Limnol Oceanogr* ,17, pp. 327–340.

Silvert, W., and Platt, T., 1978. Energy flux in the pelagic ecosystem: a time-dependent equation. *J. Limnol. Oceanogr.*, 23, pp. 813–816.

Sommer, F., Saage, A., Santer, B., Hansen, T., and Sommer, U., 2005. Linking foraging strategies of marine calanoid copepods to patterns of nitrogen stable isotope signatures in a mesocosm study. *Mar Ecol Prog Ser* ,286, pp. 99-106.

Sommer, U., and Sommer, F., 2006. Cladocerans versus copepods: the cause of contrasting top-down controls on freshwater and marine phytoplankton. *Oecologia* ,147, pp. 183-194.

Speirs, D.C., Gurney, W.S., Holmes, S.J., and 6 others, 2004. Understanding demography in an advective environment: modelling *Calanus finmarchicus* in the Norwwgian Sea. *Journal of Animal Ecology*, 73, pp. 897-910.

Steinberg, D.K., Copel, J.S., Wilson, S.E., and Kobari, T., 2008. A comparison of mesopelagic mesozooplankton community structure in the subtropical and subarctic North Pacific Ocean. *Deep Sea Research Part II: Topical Studies in Oceanography.* 55 (14-15), pp. 1615-1635.

Steward, G.F., Smith, D.C., and Azam, F., 1996. Abundance and production of bacteria and viruses in the Bering and Chukchi Seas. *Mar Ecol Prog Ser,* 131, pp. 287-300.

Straneo, F., 2006. Heat and Freshwater Transport through the Central Labrador Sea. *Journal of Physical Oceanography*, 36, pp. 606-628.

Strom, S.L., and Morello, T.A., 1998. Comparative growth rates and yields of ciliates and heterotrophic dinoflagellates. *Journal of Plankton Research,* 20(3), pp. 571-584.

Swift, J. H., 1986. The Arctic Waters. In: Hurdle G. , ed. The Nordic Seas. Berlin: Springer Verlag; 1986. pp. 130-153.

Talley, L. D., and McCartney, M.S., 1982. Distribution and circulation of Labrador Sea Water, *J. Phys. Oceanogr*., 12, pp.1189–1205.

Tieszen, L.L., Boutton, T.W., Tesdahl, K.G., and Slade, N.A. ,1983. Fractionation and turnover of stable carbon isotopes in animal tissues: Implications for $\delta^{13}C$ analysis of diet. *Oecologia* ,57, pp. 32-37.

Tiselius, P., and Jonsson, P.R., 1990. Foraging behaviour of six calanoid copepods: Observations and hydrodynamic analysis. *Mar Ecol Prog Ser* ,66, pp. 23 - 33.

Turner, J.T., Levinsen, H., Nielsen, T.G., and Hansen, B.W., 2001. Zooplankton feeding ecology: grazing on phytoplankton and predation on protozoans by copepod and barnacle nauplii in Disko Bay, West Greenland. *Mar Ecol Prog Ser*, 221, pp. 209-219.

Unstad, K. H., and Tande, K. S., 1991. Depth distribution of *Calanusfinmarchicus* and C. *glacialis* in relation to environmental conditions in the Barcnts Sea. Pp. 409-420 in Sakshaug. E.. Hopkins. *C*. C. E. & 0ritsland. N. A. ed. *Proceedings of the Pro Marc Symposium on Polar Marine Ecology*, Trondheim. 12-16 May 1990. *Polar Research 10(2).*

Vander Zanden, M. J. V., Cabana, G., and Rasmussen, J. B.,1997. Comparing trophic position of freshwater fish calculated using stable nitrogen isotope ratios ($\delta^{15}N$) and literature dietary data. *Can. J. Fish. Aquat. Sci*., 54 (1997), pp. 1142.-1158.

Vander Zanden, M. J., and Rasmussen, J. B., 2001. Variation in delta N-15 and delta C-13 trophic fractionation: Implications for aquatic food web studies, *Limnol. Oceanogr*., 46, pp. 2061–2066.

Vander Zanden, M.J., and Rasmussen, J.B. 1996. A trophic position model of pelagic food webs: impact on contaminant biomagnification in lake trout. *Ecol. Monogr*. 66, pp. 451-477.

Walter, T. C., Boxshall, G., 2014. *Microcalanus pygmaeus* (Sars G.O., 1900). In: Walter, T.C. & Boxshall, G., 2014. World of Copepods database. Accessed through: World Register of Marine Species at http://www.marinespecies.org/aphia.php?p=taxdetails&id=104513 on 2014-04-29.

Wooton, J.T., and Power, M.E,. 1993. Productivity, consumers, and the structure of a river food chain.

Proc. Natl. Acad. Sci. U.S.A. ,90, pp. 1384-1387.

Wright, W.R., and Morthington, L.V., 1970. The water masses of the North Atlantic Ocean; a volumetric census of temperature and salinity. Serial Atlas of the Marine Environment, Folio 19, *Amer. Geogr. Soc.*, 8, pp. 7-8.

Wu, Y., Platt, T., Tang, C.C.L., and Sathyendranath, S., 2008. Regional differences in the timing of the spring bloom in the Labrador Sea. *Marine Ecology Progress Series,* 355, pp. 9-20.

Yashayaev, I., and Greenan, B.J.W., 2011. Environmental conditions in the Labrador Sea in 2010. In: Northwest Atlantic Fisheries Organization: Scientific council meeting. Department of Fisheries and Oceans, Bedford Institute of Oceanography.

Yashayaev, I., and Loder, J.W., 2009. Enhanced production of Labrador Sea Water in 2008. *Geophysical Research Letters,* 36 (1), pp.1-7.

Zhou, M., 2006. What determines the slope of a plankton biomass spectrum? *J. Plankton Res.,* 28, pp. 437–448.

Zhou, M., and Huntley, M.,1997. Population dynamics theory of plankton based on biomass spectra. *Mar. Ecol. Prog. Ser.,* pp. 159, 61–73.

Zhou, M., Carlotti, F., Zhu, Y., 2010. A size-spectrum zooplankton closure model for ecosystem modelling. *J. Plankton Res*. ,32, pp. 1147-1165.

Zhou, M., Tande, K..S., Zhu, Y., and Basedow, S., 2009. Productivity, trophic levels and size spectra of zooplankton in northern Norwegian shelf regions. Deep-Sea Research II, 56 (2009) , pp. 1934–1944.

Zooplankton Identification Manual for North European Seas (ZIMNES), Microcalanus pygmaeus[online]. Available at: http://192.171.193.133/detail.php?sp=Microcalanus%20pygmaeus
(Accessed on 12 February 2014)